Escola de Camins
Escola Tècnica Superior d'Enginyeria de Camins, Canals i Ports
UPC BARCELONATECH

THEORETICAL AND EXPERIMENTAL STUDY ON MACRO-SYNTHETIC FIBER-REINFORCED CONCRETE SUBMITTED TO COOLING PROCESSES

TREBALL FINAL DE GRAU

Treball realitzat per:

Juan A. Delgado Carballo

Dirigit per:

Albert de la Fuente Antequera

Pablo Pujadas Álvarez

Grau en:

Enginyeria d'Obres Públiques

Barcelona, Setembre 2017.

Departament d'Enginyeria de la Construcció

Abstract.

Theoretical and Experimental Study on Macro-Synthetic Fibre-Reinforced Concrete Submitted to Cooling Processes

Author: Delgado Carballo, Juan Andrés

Tutors: de la Fuente, Albert y Pujadas Alvarez, Pablo

When precast concrete used for TBM tunnel segments is submitted to cooling processes (due to the temperature gradient between the concrete and the environment in which it is set to cool), thermal deformations are bound to appear. These deformations, however, aren't usually enough to affect concrete behaviour drastically. The scenario changes when temperature, humidity and other climate factors are severe: great temperature gradients, among other factors, are bound to produce differential thermal shrinkage thus producing tensile stresses in concrete elements and, consequently, appearance of cracks.

The aim of the present thesis is to analyse how Plastic-Fibre-Reinforced-Concrete (PFRC) behaves in the previously mentioned cooling phases in order to study the ability of macro-synthetic fibres to bridge potential cracks in external faces of the concrete elements.

For this purpose, an experimental campaign was carried out with PFRC specimens in order to obtain and analyse mechanical traits of the elements in question, including residual flexural strength which would help understand cracking behaviour.

Resumen.

Estudio teórico-experimental de hormigones reforzados con fibras sometidos a procesos de enfriamiento.

Autor: Delgado Carballo, Juan Andrés

Tutores: de la Fuente, Albert y Pujadas Álvarez, Pablo

Cuando el hormigón prefabricado utilizado para fabricar dovelas de túneles se somete a procesos de enfriamiento (debido al gradiente de temperatura entre el hormigón y el ambiente al que está expuesto), aparecen deformaciones térmicas. No obstante, estas deformaciones no suelen ser lo suficientemente graves como para causar daños notables al comportamiento del elemento. El escenario cambia cuando ciertos factores climáticos (temperatura y la humedad entre otros) se presentan de manera severa: grandes gradientes de temperatura, entre otras causas, provocará muy probablemente retracción térmica diferencial, provocando tensiones de tracción en las caras externas de los elementos y, a su vez, produciendo fisuras en los mismos.

La respuesta de hormigones reforzados con fibras de plástico (HRFP) en régimen de enfriamiento y bajo temperaturas reducidas es aún desconocido. En este trabajo de investigación se pretende caracterizar el comportamiento del HRF en fase de enfriamiento con el fin de estudiar la capacidad de las fibras para coser potenciales fisuras en las caras externas de los elementos.

Por este motivo, se ha llevado a cabo una campaña experimental en la que se han ensayado probetas de hormigón reforzado con fibras plásticas con tal de analizar la respuesta mecánica de los elementos en cuestión, incluyendo la resistencia residual, la cual juega un rol importante en predecir el comportamiento antes fisuras del hormigón

Index.

List of Tables.

List of Figures.

CHAPTER I

1. Introduction & Objectives

5.1. Introduction

In Construction Engineering, there is constant research for new materials which are able to meet the requirements of structural stability or durability that technological advances require. One of these relatively new materials that has been gaining weight for the past decades in this industry is Fiber Reinforced Concrete (FRC). FRC is one of the most relevant innovations in the special concrete field. These types of concrete are mainly characterized by including short fibers distributed randomly in its mix.

The addition of fibers to the mix modifies the non-linear behavior of structural concrete, especially in traction, impeding the opening and propagation of cracks. Once the concrete cracks, the contribution of tensile strength due to the bridging effect of the fibers, improves the residual strength of the composite material. Consequently, and thanks to the *debonding* (loss of grip) and the pull-out mechanism of the fibers, a greater amount of energy is dissipated, leading to an important rise in tenacity and a better control of cracking.

The types fibers that are added to the mix logically determine the behavior the composite material will have once it is in service. In this matter, this thesis studies the behavior of Plastic Fiber Reinforced Concrete (PFRC).

PFRC has normally been used in pavements and underground constructions. The fibers in these cases were strictly applied for durability purposes, mainly to control cracking in early and late phases of the structure. In other words, the structural contribution from fibers to the structure wasn't contemplated at the time.

During the past years, the use of plastic macro fibers with a high elastic modulus has started to stand out. These plastic macro fibers are structural, meaning they contribute in resistance of the material and, even though their efficiency cannot be compared to that of the steel fibers, are a very interesting solution in modern day projects. Plastic fibers have the advantage of being chemically inert and very stable in alkaline environments (as is concrete). These characteristics and the lower cost of the fibers in comparison to the other types make it not only a structural viability, but a more economical option in projects.

To this day, most state of the art in FRC has been study-oriented towards steel fibers and not as much towards plastic (polypropylene) fibers. The mechanical behavior under critical temperatures in traditional reinforced concrete has been thoroughly investigated and tested, providing codes that dictate how a specific structure will behave under certain temperatures. These types of guidelines do not exist, however, for PFRC.

5.2. Context

Concrete reinforcement design for tunnel linings must take into account many factors which include the stresses the element will suffer once its submitted to stress states. One of these stress states, and main theme in this thesis, is the cooling down process when extreme gradient temperatures are present (see Figure 1). These stress states are almost prone to causing strong tractions on the external fibers and compressions on the inner part of the section (Figure 2).

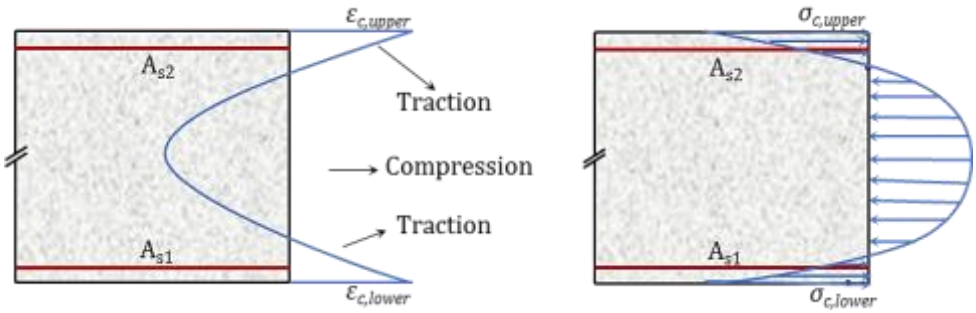

FIGURE 1. INNER RESISTANT MECHANISM OF THE CROSS-SECTION DUE TO DIFFERENTIAL THERMAL ACTION

In this line of study, tunnel linings being built in countries which can harbor these climate conditions (e.g. Norway, Canada) should take the consequences into account in order to obtain a proper concrete reinforcement design.

Although tunnel linings are mostly submitted to compression once they are placed in their final position, these structural elements will suffer large external stresses due to the low temperatures to which they will cool down in their fabrication process (Figure 3).

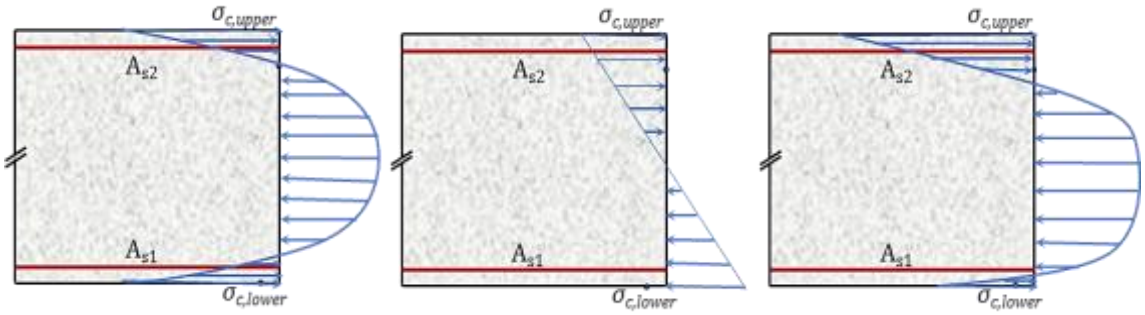

FIGURE 2. TENSIONAL MECHANISMS: (A) SELF-TENSION DUE TO DIFFERENTIAL THERMAL RETRACTION; (B) STRESS DUE TO ITS OWN WEIGHT (C) TOTAL STRESS STATE

FIGURE 3. DEMOLDING OF TUNNEL LININGS

Regarding the temperature, given the extreme gradient, temperature of the external fibers will reach environment temperature much faster than the internal fibers. This temperature gradient leads to the heat transfer process, the retractions of which are considered as non-uniform and generates internal tension due to the Navier-Bernoulli hypothesis (two initially flat and parallel cross sections remain flat but not parallel throughout the deformation process, even in the plastic region).

Given the internal stresses that are present in the element, cracks are prone to appear in the external fibers (submitted to traction) if the tensile strength of the concrete is exceeded. This of course, is sure to be accompanied by stresses that appear in the stacking process (Figure 4) and those related to the differential retraction during the cure of the elements.

FIGURE 4. TUNNEL LINING SEGMENTS PLACED IN STORAGE PARK

5.3. Objectives

Fiber-reinforced concrete in in cooling processes and low temperature regimes is still unknown. This investigative thesis aims to:

(1) Characterize behavior of plastic fiber reinforced concrete in cooling processes for the purpose of studying the capacity fibers possess for sewing potential cracks in the external faces of the element.

(2) Study the tensile embrittlement of this type of concrete once it is submitted to different levels of freezing temperatures.

Keeping this in mind, this study could possibly be innovative in this field of study, helping at the same time the use of PFRC in countries with similar weather to the ones described in the present thesis.

As mentioned previously, most state of the art is study-oriented into steel FRC which even though it has a similar application and way of acting, behaves significantly differently mechanically and in other aspects. This thesis could impulse the study of PFRC as a main subject, instead of including it consistently in SFRC studies.

5.4. Roadmap of the Thesis

The present Bachelor Thesis consists of five chapters (Figure 5), the first one being the present introduction. This introduction has the aim to introduce the reader to the field of study discussed in the document, as well as a general outlook of the goals intended by the research.

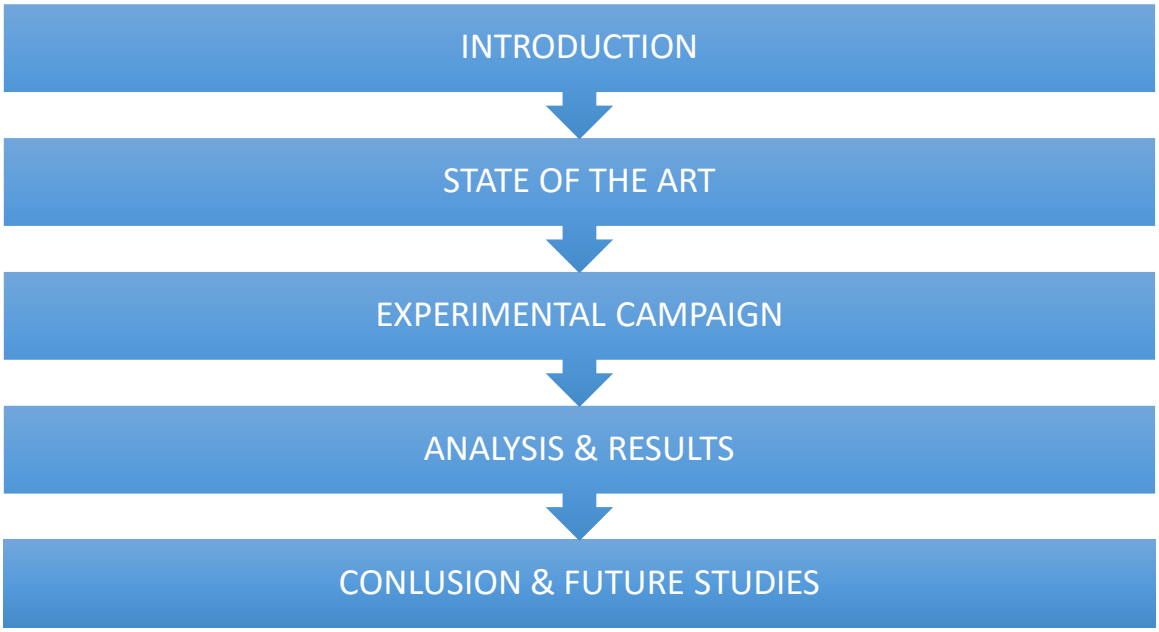

FIGURE 5. OVERVIEW OF THESIS ORGANIZATION

After the introduction comes the state of the art. This chapter is intended to summarize briefly the most relevant knowledge about PFRC and their main properties as well as most relevant codes that allow the definition of the constitutive equations and tests for the characterization of FRC.

The third chapter covers the details related to the experimental campaigns that have been carried out for the study. These details include aspects such as optimal dosing, proper methodology for the production of the concrete specimens or tests to characterize the before mentioned mechanically.

Analytical results are found in chapter four. These results, fruit of the experimental campaigns mentioned in the third chapter, allows us to evaluate the positive (or negative) influence of freezing temperatures in PFRC. Furthermore, the results are also compared to those of PFRC in room temperature, enabling the comparison of the most critical differences.

The Thesis concludes with chapter five, which covers the most relevant conclusions that derive of the experimental campaigns undertaken as well as the future studies proposed.

CHAPTER II

2. State of the Art

2.1 Introduction

Macro-Fiber-Reinforced Concrete (FRC) is a composite material, whose use in precast concrete leads to an improvement in its mechanical behavior (Kim 2011) by increasing its tenacity (Zheng 1995), its fire resistance (Blontrock 1999), its impact strength (Bayasi 1993) and towards stresses (Alhozaimy 1996) that may appear during transitional phases. Technological advances in the field of study related to fibers, has uncovered the possibility of completely replacing conventional reinforced concrete in tunnel segments for Fiber-Reinforced concrete. In this context, such substitution could be an interesting approach in terms of concrete fabrication and their benefits in tunnel segments, due to its intrinsic advantages, like the simplification in the framework mechanism thanks to the absence of the need for vibration, the decrease in execution time or the decrease in acoustic contamination, among others.

Use of macro plastic fibers to reinforce concrete has attracted widespread attention from both scientists and construction industry due to the multiple sustainability benefits they offer, compared to steel fibers and steel reinforcing mesh (Wang, 1998) .

The term “macro plastic fibers” evidently references the category type of the plastic fiber. All fibers are put into two main groups: Micro-Fibers or Macro-Fibers, the latter being the subject of this thesis and having lengths between 19 and 60 mm. They are in turn expected to sew the cracks that form on the element and provide it with structural support once concrete has hardened. Micro-Fibers, on the other hand, are added to the concrete mix in order to help the fresh state of the concrete and the early-age tensile and flexural strength of concrete (G Zhou, 2002)

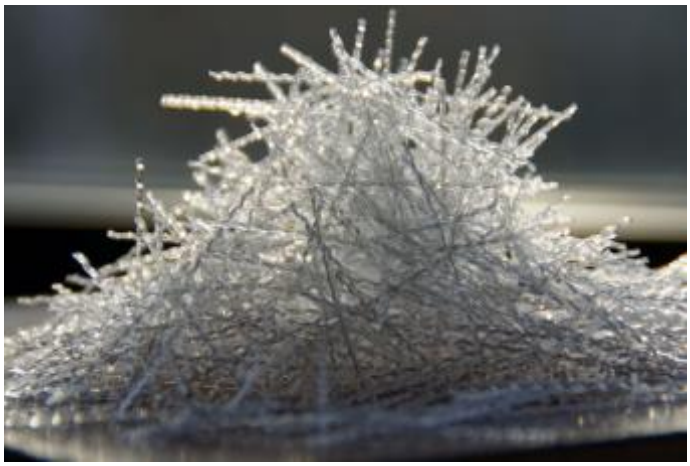

FIGURE 6. MACRO-SYNTHETIC PLASTIC FIBERS

Typical applications of concrete with Macro-Plastic Fibers range anywhere from industrial pavements to tunnel linings (Belleti B, 2008) thanks to their favorable mechanical properties and the economic advantage they possess regarding conventional reinforced concrete.

These macro-fibers can be fabricated using different types of materials, as can be seen in the figure below, and are used in function of their characteristics and the use they are intended to. However, Polypropylene is one of the most used synthetics is fibres for concrete. This is due to their light weight and relative low cost (Manolis, 1995).

Currently, FRC has been used in a great variety of applications: pavements, aircraft parking, slope stabilization, dams and hydraulic structures, and tunnel lining among others (Zollo, 1997). Steel fibers have been throughout the last decades the main type of fiber used in these types of projects (Soutsos, 2012) thanks to their similar mechanical properties in comparison to traditionally reinforced concrete, and to its economic advantages. When it comes to tunnel linings, the behavior of these steel fibers under extreme temperatures has become a concern. An alternative to steel fibers in this type of structural application is Plastic Fibers: Plastic-Fiber-Reinforced Concrete (PFRC), has been the target of a great amount of research projects over the last years and has consequently gained popularity in the structural field, contributing to certain structural characteristics that steel fibers lack.

In this chapter, three different parts will be analyzed for their state of the art. At first, a general vision of Plastic-Fiber Reinforced Concrete (PFRC) will be presented with recent developments and technological advances in this field of study, as well as characterization method regarding these types of fibers.

	Specific gravity	Tensile strength (Mpa)	Elastic Modulus (GPa)
Acrylic	1.16-1.18	296-1000	14-19
Aramid I	1.44	2930	62
Aramid II	1.44	2344	117
Carbon I	1.9	1724	380
Carbon II	1.9	2620	230
Nylon	1.14	965	5
Polyester	1.34-1.39	228-1103	17
Polyethlene	0.92-0.96	76-586	5- 117
Polypropylene	0.9-0.91	138-690	3.0-5.0
Alkali-resistant	2.7-2.74	2448-2482	79-80
Non Alkali-resistant	2.46-2.54	3103-3447	655-72
Coconut	1.12-1.15	120-200	19-26
Sisal	-	276-568	13-26
Bagasse	1.2-1.3	184-290	15-19
Steel	7.8	1000-3000	200
Glass	2.6	2000-4000	80

TABLE 1. DIFFERENT TYPES OF SYNTHETIC FIBERS AND THEIR CORRESPONDING SPECIFICATIONS

The second part of this chapter consists of a balance of the main characteristics that steel fibers and plastic fibers provide (or lack), with tunnel segments being the main objective of the comparison.

Lastly, the third part of the chapter will be dedicated to the behavior of FRC used in precast tunnel linings subjected to the extreme temperatures that are likely to occur in some countries with far-sub-zero temperatures.

2.2 Plastic-Fiber-Reinforced Concrete

Over the last few years and due to advances in experimental campaigns and research projects, new fibers have been developed with an ability to adequately reinforce concrete, avoiding the use of a metallic mesh and allowing a substitution of traditionally reinforced concrete with rebar in determined conditions (Di Prisco, 2009).

According to EHE 08: *Fiber-Reinforced Concrete,* is defined as concrete that includes short, discrete and randomly distributed fibers in its composition. Fibers have evolved from

its main application as polymeric micro-fibers (defined as fibers no larger than 0,30 mm) to improve concrete properties such as plastic shrinkage cracking (mainly in pavements) or fire resistance (specifically in tunnel linings, improving its passive protection against fire). These micro-fibers, however, are not employed with a structural purpose, given they do not modify concrete's mechanical properties (Lawler, 2005).

Similarly, steel fibers have in the past contributed in developing a structural point of view in FRC. New testing methods have permitted their structural capacity evaluation Mainly FRC increases ductility of the matrix by increasing residual tensile strength in bending and increases energy absorption (Wafa, 1990).

Through the emergence of synthetic polymeric fibers with structural capacity (currently covered in EHE-08 Instruction: Annex 14), new possibilities emerged that can outsource steel fibers in certain aspects. Similar steel fibers and upon having possibilities of being considered as structural reinforcement, these fibers have seen other aspects in which their use could be considered beneficial in regards to steel fibers (Buratti, 2011).

2.2.1 APPLICATIONS

Though in the near future the use of Macro-Synthetic FRC will mostly be common for the majority of applications, currently their use has been mainly focused on:

- Sprayed Concrete and Mortar. These are mainly used in soil stabilization, swimming pools and in underground structure stabilization (tunnels, caves or mines) (Johnston, 2010).
- Concrete Pavements, where there is a broad experience with steel fibers and thus the fiber-reinforced system is well known by engineers in this field (Johnston, 2010).
- Precast Concrete. These can include enclosing panels and retaining walls, complex architectural pieces or generally any concrete piece which requires a strong bi- and tri-dimensional reinforcement, provided by the fibers acting almost as an isotropic material (Caratelli, 2011).
- Floor Slabs. FRC is being used more every time as an appropriate system to redistribute stresses in compression layers in slabs. (Ritter, 1995)
- Other types of applications: for concrete submitted to aggressive environments, near sea, etc. (Ramli, 2013).

2.3 Why Macro-Plastic Fiber Reinforced Concrete?

When precast tunnel linings are manufactured, they undergo certain phases in which their performance may be affected. These phases are mainly the handling process and the curing process.

In the handling phase, segments are removed from their corresponding framework and then handled. This basically refers to the manipulation carried out once it is taken out of the cast and until it is in the precast park in its curing process. In the images below, segments are handled once they have been removed from the cast and transported by crane to the storage park.

FIGURE 7. DEMOLDING (A) AND HANDLING (B) OF PRECAST TUNNEL SEGMENTS.

In the curing process, segments are stacked in a pile where they will cool down, in which they will suffer stresses due to self-weight and thermal retraction, among others.

FIGURE 8. STACKING OF PRE-CAST TUNNEL LININGS.

The possible cracks due to thermal retraction (in turn due to the high temperature gradient) is what makes this phenomenon so crucial and why it is also the main subject of the thesis.

Tunnel segments undergo a specific curing process called steam curing. Steam curing is a form of curing in which the elements are placed in a chamber with a specific temperature, humidity and pressure controlled by a panel. Heat and moisture penetrate the materials quickly to fully hydrate and harden them. This process is done in order to gain an early strength sufficient to withstand the stresses they will suffer in early stages. The process all segments undergo, regarding temperature and time, can be observed in the graph below.

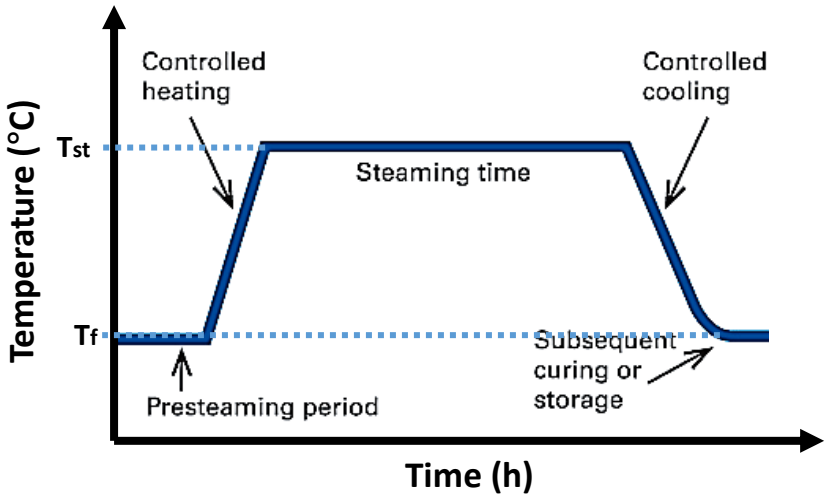

FIGURE 9. STEPS IN STEAM CURING PROCESS

During controlled heating, the segments are heated for the process at a uniform rate of approximately 10ºC/hour, which aims to avoid extreme temperature variations. This method is repeated again for controlled cooling with similar cooling rate (5-10ºC/hour).

In order to help prevent cracking due to these previously mentioned factors, macro-fibers are used to help bridge these cracks and enhance durability and abrasion resistance among other mechanical properties. Experimental results indicate that FRC is more effective in crack reduction than plain concrete. It was found that plastic shrinkage cracks were significantly reduced with addition of plastic fibers, compared to steel FRC and plain concrete. (Grzybowski, 1990)

Furthermore, results showed the better behaviour of concrete reinforced with steel fibres in terms of toughness, while FRC with synthetic fibre showed a good behaviour in terms of reduction of shrinkage cracks (Cominoli, 2007). Given certain applications (e.g. tunnel linings where segments are not primarily subjected to other stresses than compression)(de la Fuente, 2015), this could allow the adoption of plastic fibers instead of steel

There are several factors and circumstances that define the capacity of energy absorption (i.e. ductility) that we can classify according to different criteria. If we focus on type of concrete we would find factors such as type of cement, size of the aggregates, w/c ratio, etc. If, instead, we focus on the type of fibers we can distinguish between the following factors:

2.3.1 Quantity of fibers in volume

The amount of fibers that are added to the mix per cubic meter of concrete influences the energy absorption establishing direct relationship between them: So that, the more quantity of fibers in the mix per cubic meter, the more ductility and energy absorption the concrete will present. (Soroushian, 1990)

2.3.2 Tensile resistance and adherence

FRC may fracture due to loss of adherence (pull-out mechanism) or by the breaking of the fiber. For this, both variables also play a role simultaneously in the capacity of energy absorbed. In other words, a fiber with great amount of tensile resistance may not increase its ductility if this resistance is not proportional to the adherence. (Shah, 1971)

2.3.3 Size and shape

The length of the fiber acts upon the flexural resistance that the concrete will present, establishing proportionality between both variables so that more length would equal more flexural resistance, although special project necessities or execution constraints must be taken into account.

Shape influences principally in the adherence of the fibers to the matrix (Al Qadi, 2014). Circular-section fibers present less adherence than flat-rectangular fibers. This is due to the contact area being lower in circular type fibers than in the flat ones, which is why their surface must be modified (rugged surfaces, angular borders, etc.)

2.3.4 Comparison of Steel Fibers and Plastic Fibers

Given the lower density of polypropylene (0.91 g/cm^3) (*Efs-plastics.ca*) against that of steel (7,85 g/cm^3), the amount of polypropylene fibers in, for example, 1kg of FRC will be greater than the amount of steel fibers in the same 1kg of FRC. This means that in terms of fiber volume, less fibers need to be used for the same result.

Another important component which plays a very important role in concrete behavior is adherence. Adherence is an essential component that plays a very important role in concrete behavior. Steel fibers have two main factors that help improve their adherence with the other components of the concrete. On the other hand, plastic fibers

apart from having these two factors, can be coated in chemical products that enhance the interaction between them. (López-Buendía, 2013)

FIGURE 10. DIFFERENT SHAPES FIBERS CAN BE FABRICATED INTO (SOURCE: BEKAERT)

When it comes to evaluating any infrastructure and, especially tunnels, durability and maintenance of their properties during their life-span is a vital factor. Steel fibers conserve their properties as long as they're covered inside the concrete. Given its acid pH that protects them against external environmental factors that could cause rust and thus a loss of their main properties might occur. This oxidation, however, can be caused by common reasons such as micro-cracks (by which water and air can penetrate producing oxidation) or by carbonated concrete (which would decrease concrete's pH and therefore causing corrosion and oxidation in the steel fibers) among others. (Granju, 2005)

Polypropylene fibers, on the other hand, do not present these corrosion and oxidation handicaps that steel fibers thus they are also more stable towards any chemical attack and increases durability of the structure. (Zollo, 1997)

For the same perspective of durability, fire resistance is a very important characteristic concrete must possess. When concrete is exposed to elevated temperatures like the ones apparent in a fire, the water present inside the concrete evaporates, producing stresses that cause crack and breakage of concrete. This phenomenon is because it is not able to release produced stresses. This effect could lead to *spalling*, making it possible to result in an explosive rupture in some cases. (Poon, 2004)

When synthetic fibers are added as a reinforcement, this phenomenon becomes much less likely to happen, thanks to the cavities that these fibers leave behind once they are liquated by the elevated temperatures creating internal canals which help release inner stresses (Peng, 2006). However, steel fibers do not present this advantage and, even counter-productively, they worsen the cause given the different expansion coefficient of concrete and steel, which do not relieve the before-mentioned stresses. (Peng, 2006)

It is well known that macro-synthetic plastic reinforced concrete is more efficient than plain concrete regarding elevated temperatures, but little is known about the behavior these possess under extreme low temperatures, which brings this chapter to its final part: Behavior of Plastic Fiber Reinforced Concrete Under Freezing Temperatures. (Zheng, 1995)

2.4 Behavior of PFRC Under Freezing Temperatures

The question remains that how will PFRC behave or perform once temperature has lowered up to sub-zero temperatures. From another perspective, it is still unresolved to know how a great temperature differential (up to -40 ºC) will affect PFRC mechanical properties. The writing of this thesis, being the main focus of this thesis while it has not been yet studied by investigators, aims to answer these uncertainties.

To achieve these goals, some investigations and researches that have been performed through plain concrete and plastic materials might be used. Such information helps the writer to better predict some behavior of the composite material.

2.4.1 Plain Concrete

Freezing resistance is greatly influenced by the humidity that concrete possesses. It is in fact the amount of water inside the pores that can freeze. This phenomenon alters the mechanical properties of this concrete mix. Under certain temperatures, not only do we have colder concrete, but a system formed by ice and concrete that exhibits great advantages in some applications. For this reason, for some temperatures, compressive resistance can be up to three times greater than at room temperature. Similar effects can be observed with concrete deformation due to the great resistance that ice contributes to and the micro pre-stress that water creates as it freezes. (Elices Calafat, 1981)

During the freezing process, water transforms into ice in different phases. Depending on which substances are dissolved in them, water stored inside the bigger pores starts freezing at 0 to -10 ºC. Then, water condensed inside capillary pores start freezing at -30 to -80 ºC. Finally, water absorbed by the walls of the smallest pores can freeze at about -160 ºC. Consequently, when concrete freezes, it maintains a gradient transition in which ice, water and steam are coexisting simultaneously during a broad interval of temperatures.

Concerning tensile resistance, the tensile strength tends to diminish as humidity lowers and increases as temperature decreases. When -100 ºC is reached, the strength tends to decrease instead of stabilizing, which is in contrary to the compression resistance. This factor, however, does not concern this thesis as temperatures will not be lower than -30 ºC in any case.

Concrete Resistance Under Subnorma Temperatures

	Compression Strength		Tensile Strength	
Age	28 days	22 months	22 months	22 months
Temperature	-165 ºC	-196 ºC	-196 ºC	-196 ºC
Humidity	5,50%	2%	7%	2%

TABLE 2. CONCRETE RESISTANCE UNDER SUBNORMAL TEMPERATURES

2.4.2 Plastic Fibers

Temperatures below 0 ºC can be harmful for plastics because they do not conserve their same familiar properties of flexibility and high resistance to cracking that they show in room temperature. This can lead to a brittle type of behavior with low failure stresses. Consequently, behavior under freezing temperatures must be thoroughly evaluated before exposing this material to the critical environment.

The glass transition temperature (Tg) can be defined as the temperature under which plastic fibers stop behaving as a 'rubbery' material and start stiffening, becoming very hard and thus very brittle. Typically, once plastic fiber is exposed to temperatures below Tg, no other transitions occur and it becomes 'stable'. Therefore, if low temperatures were to be analyzed generally, they would not necessarily be benign for FRC since generally their impact resistance is significantly decreased and the principle failure mechanism becomes brittle failure.

Tg varies greatly depending on the plastic in question, as well as the base polymer's specific molecular structure. For Polypropylene, main components of the synthetic-type fiber used in the experimental campaign this thesis discusses, Tg can be estimated to be approximately -20 ºC but, as previously mentioned, this temperature can vary due to the different additives used in its fabrication or other factors.

In experimental campaigns, therefore, it would be interesting to define the specific Tg of the polypropylene-based fibers, for if the glass transition temperature is lower than the temperature for which they are intended, the consequences of such temperature won't be as critical than in other cases.

2.4.3 Deformation Under Low Temperatures

Knowledge on how a structure will deform due to thermic causes is essential in order to design infrastructures that will be exposed to extreme temperature fluctuations. It is known that plain concrete, when cured and stored correspondently in optimal conditions, shows a mainly linear and reversible behavior (mostly dependent on the aggregate curve). On the contrary, saturated concrete shows a non-linear behavior and thus irreversible which, according to Elices Calafat can be divided into three regions:

- Between 20 ºC and -15 ºC, concrete contracts.
- Between -20 ºC and -60 ºC concrete expands. This is called the transition region and can be explained by taking into account the gradual transformation of water into ice on concrete pores.
- Under -70 ºC contracts once again.

When concrete expands under -20 ºC, it depends on how fast the temperature transitioned. This is believed to happen given that fast freezing impedes re-accommodation of water particles, which generates great pressure. Irreversible deformations also increase with freezing velocity.

In the following graph, it can be observed how saturated concrete reacts regarding temperature and deformation.

For this thesis, the temperatures that would affect the experimental campaign would be those ranging from 20 ºC down to -30 ºC approximately. This would mean that during certain temperatures, we could see how the effect of contraction (until -15 ºC) or expansion (below -20 ºC) influences on the tests

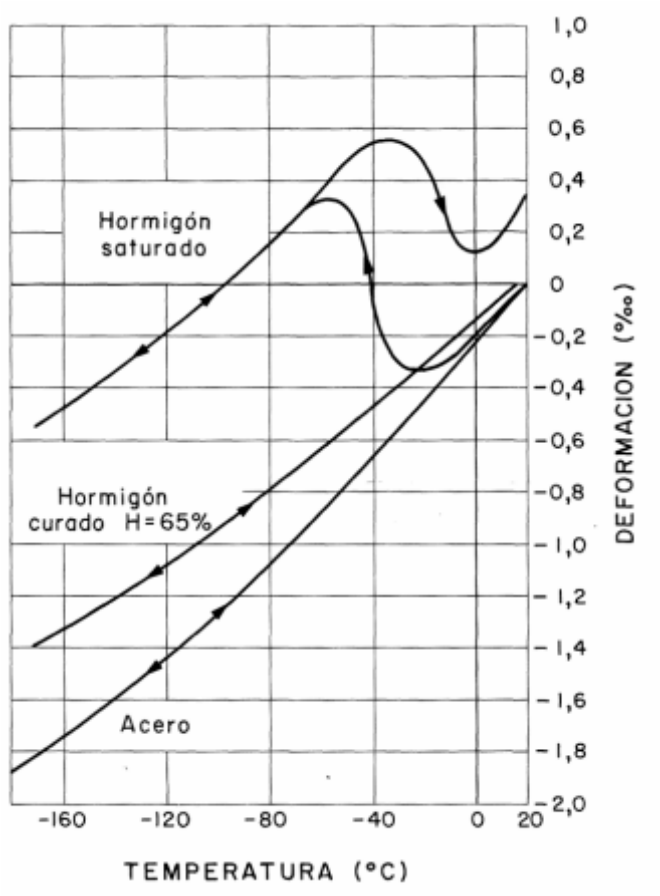

FIGURE 11. RELATION BETWEEN TEMPERATURE AND DEFORMATION (M. ELICES, 2005)

CHAPTER III

3. Experimental Campaign

3.1 Introduction

This chapter introduces the methodology used in the research framework of the DURADOV project. This project, which consists in the *development of non-metallic fiber-reinforced concrete of elevated durability and improved sustainability*, is a state-wide R&D project oriented towards construction challenges. It is leaded by the company DRAGADOS and includes the UNIVERSITAT POLITÈCNICA DE CATALUNYA as research organization through the GRUPO DE INVESTIGACION DE TECNOLOGÍA DE MATERIALES Y ESTRUCTURAS.

Given that this research project could lead to using non-metallic FRC in the construction of tunnel segments in countries with extremely low temperatures like Norway or Canada, the behavior that the type of concrete can undergo under these circumstances is of great concern.

For the planning of the experimental campaign, DURADOV consisted of three phases in which different types of doses, content of fiber in volume and fiber types were used. This was done in order to emphasize the influence that each of these parameters had on the behavior of the concrete. The present thesis focuses on the final dose used in the project and how freezing temperature affects it's mechanical and physical behavior.

In order to comprehend the behavior that PFRC will have under these temperatures, the specimens were exposed to freezing temperatures and then tested for characterization.

3.2 Objective

The objective of this chapter is to acknowledge the methodology that was used for the specimen elaboration, with the intention to subsequently test them.

Making an elaborate description of the methodology and the experimental campaign is a key component so that future studies in the same realm can have a reference and consequently saving time and gaining efficiency. This description which is included in the majority of research projects, rigorously describes the most important steps that have been taken during the experimental campaign.

In order to facilitate the comprehension of the results obtained in the following chapter, the following sections will be covered:

- Campaign Planning
- Material & Dosage
- Concrete Fabrication Procedure & Specimen Elaboration
- Fresh and Hardened Concrete Tests

3.3 Campaign Planning

Campaign planning is what basically gives the experimental campaign the organization it requires towards specimen elaboration and testing.

In this first phase, we aim to determine the tests that will be needed in order to understand the behavior we intend to grasp information on, those which are carried out on fresh concrete and those on hardened concrete. In addition, the number of specimens for each dose, temperatures and their dimensions are also included.

In order to characterize PFRC, different types of tests are useful. First, when concrete is in its fresh state, the amount of **occluded air** (microscopic bubbles of air trapped inside the concrete mix during the stirring), its **consistency** and its **density** are characteristics that are to be determined.

The other test needed in order to be able to characterize the behavior of the concrete specimens was carried out once it had reached its hardened state. This test is the **Three-Point Bending Test** [UNE-EN 14651] and it consists in fracturing the concrete specimen by applying a load in the center while supporting the specimen through two pins in each opposite side. To adopt a controlled fracture, the specimens included a single notch

transversally along the center of the specimen, opposite to the side where the load was to be applied. This notch evidently created a segment with less resistance that was prone to fracture before the rest of the specimen.

Furthermore, as a means of determining behavior of the specimens in these extreme temperatures, the concrete specimens were frozen to three different temperatures prior to being tested in their hardened state: **-30 ºC, -20 ºC and -10 ºC**. Not only did this provide information on different temperatures but it also allowed for determining transition phases in referral to its temperature.

3.4 Materials & Dosage

For the present campaign, material selection and dosage was evidently crucial and had an elaborate study backing it up. A brief description of the materials used and their importance in behavior is included in this chapter in order to better understand its components.

3.4.1 Water

Water is evidently a very important substance that influences concrete fabrication given its conglomerating effect when mixed with cement, uniting the aggregates with the matrix. Furthermore, the quantity of water used determines workability of concrete, which increases with the amount of water added but, in turn, decreases resistance and durability.

3.4.2 Aggregates

For the concrete fabrication, three different fractions of aggregate of different type of limestone were considered. The first fraction is composed by sand with 0/4 mm diameter, 4/10 mm diameter earth for the second fraction and lastly a diameter of 10/20mm od gravel for the third and last fraction.

The aggregates come from PROMSA's quarry in PALLEJÀ and their maximum diameter, $D_{max} = 20mm$. The following table summarizes the specific weights for the different types of aggregates:

Aggregate	Specific Weight [kg/dm^3]
0/4mm	2,66
4/10mm	2,57
10/20mm	2,58

TABLE 3. AGGREGATE SPECIFICATIONS

3.4.3 Cement

The cement used in this experimental campaign consists in a High-Resistance Portland cement (CEM I/52,5 R) and is delivered by “Ciments Molins”.

3.4.4 Additives

The additives that were used in experimental campaign consist of a super-plasticizer (**MasterGlenium Sky 886**) and a setting accelerator additive.

MasterGlenium Sky 886 was used in order to improve the workability of concrete due to low water/cement ratios. This additive, a part from the above-mentioned improvement, has the benefit of not altering the setting time of the concrete.

The setting accelerator additive provides an increase in the setting time and, therefore, the cure time starts earlier, speeding up the initial resistance of concrete as well.

3.4.5 Fibers

Lastly, the main element used in this experimental campaign in terms of significance are the fibers. As it was mentioned before, these are non-metallic type fibers, which have different origins: polyolefin derivatives, polymeric, basalt, glass fiber, glass reinforced polymeric fibers and carbon fibers. In this campaign, however, the three types of fibers used are Polyolefin based: **Barchip 48**, **Barchip 60** and **TUF-STRAND SF**.

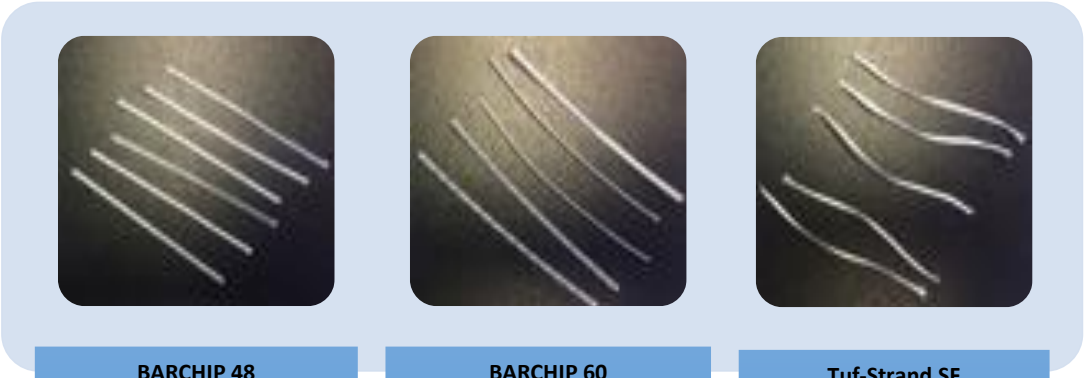

BARCHIP 48
Supplier: Elasto Plastic Concrete EPC
Material: Polyolefin
Traction Resist.: 640 MPa
Length: 48 mm
Diameter: 0,91 mm
Aspect (l/d): 53
Nº Fibers/kg: 59500
Density: 1000 kg/m3

BARCHIP 60
Supplier: Elasto Plastic Concrete EPC
Material: Polyolefin
Traction Resist.: 640 MPa
Length: 60 mm
Diameter: 0,48 mm
Aspect (l/d): 125
Nº Fibers/kg: 33000
Density: 1000 kg/m3

Tuf-Strand SF
Supplier: Euclid Group Eucomex
Material: Polyolefin
Traction Resist: 650 MPa
Length: 51 mm
Diameter: 0,66 mm
Aspect (l/d): 77
Nº Fibers/kg: 50000

FIGURE 12. FIBERS USED IN EXPERIMENTAL CAMPAIGN

Lastly, for every type of fiber mentioned in the previous illustration, a High Resistance type concrete specimen was made with different fiber content. The codes used are mentioned in order to reference the concrete batch, shown consecutively below.

Concrete Type	Fiber Type	Fiber Content (kg/m3)	Code
High Resistance Concrete	Barchip 48 EPC	10	AR_10_PP4
	Barchip 60 EPC	10	AR_10_PP5
	Tuf-Strand SF EUCLID	10	AR_10_PP7

TABLE 4. CHARACTERISTICS OF THE FIBERS USED IN EXPERIMENTAL CAMPAIGN

The “AR” nomenclature corresponds to High Resistance Concrete (Alta Resistencia in Spanish). The number that follows corresponds to the fiber content in kg/m3. Lastly, the

last figure corresponds to the fiber type; in this campaign, as it was mentioned before, corresponds to Polyolefin “PP”.

3.5 Concrete Fabrication Procedure and Specimen Elaboration

The different concrete mixes elaborated for this experimental campaign were carried out in PROMSA, a concrete-producing company in MOLINS DE REI.

In this company, and for the fabrication of all the concrete specimens, vertical axis mixers of 150 L capacity were used. The capacity of the mixer used, however, was approximately 100 L, which was used to cast the specimens planned to be tested once the concrete hardened and also allowed samples to be taken for the fresh concrete tests.

The Fabrication process carried out, as well as the order in which the materials were introduced into the mix, are summarized hereunder and explained consecutively:

Action	Mixing Time
1. Introduction of aggregate into the mixer	30 seconds
2. Introduction of the cement	30 seconds
3. Introduction of the water (set aside 1L for the introduction of the additives).	1 minutes
4. Introduction of the additive little by little with the water that was previously set aside.	2 minutes
5. Introduction of the fibers, avoiding introduction of large joints at once, into the mixer	4 minutes
6. Conduct the concrete slump test	[-]

TABLE 5. STEPS TAKEN IN CONCRETE FABRICATION PROCESS

For the fabrication process, the raw material portions that compose concrete (aggregates, cement, water and additives) were first weighed. For the amount of water, 1

kg was separated from the total and put in a small container. This was later used to be able to dilute the additives in the kneading process.

Next, the raw material is poured into the mixer, which has four mixing arms to facilitate the homogeneous mix of the materials. Gravel and sand are the first to be poured and mix during 30 seconds. After the aggregates, the cement is introduced and mixed during 30 seconds as well. The water (except the 1kg separated previously) is then poured inside the mixer and mixed during one more minute.

FIGURE 13. 4-ARM CONCRETE MIXER

Afterwards, super-plasticizer additive (Glenium TC 1425) is added to the mix (Figure 14) with the part of the 1 kg of water set aside before-hand and mixed during one minute. The rest of the water that was set aside is then poured into the mixer along with the setting accelerator (X-Seed) for another minute.

FIGURE 14. INTRODUCTION OF SUPERPLASTICIZER INTO THE MIXER

Last, the fibers are then added and mixed during 4 minutes. This has to be done carefully as the fibers have to be as much equally separated in the mix as to avoid different resistance measures along the specimen. This is done by avoiding burrs (or large concentrated amounts of fibers) poured at the same time

Once the mixer has stopped running, a small sample is removed in order to check the workability of such concrete via the slump test [UNE 83313]. If the desired consistency is reached, the molds can then be filled up.

The specimen elaboration process was done according to the normalized process UNE-EN 12390-2. Before filling the molds, the interiors are covered with a non- reacting release agent in order to avoid the concrete adhering to the mold. Next, the molds are filled up with the help of a metallic spoon. As the mold is being filled, several strokes are given to the lateral sides in order to compact the existing concrete and eliminate occluded air in the interior of the mix. This process is repeated until the mold is completely full. The residual concrete on the upper part of the mold is then eliminated using a steel trowel until the surface is perfectly smooth and levelled. It is worthwhile mentioning that specimens are then labelled in order to keep track of when they were elaborated.

FIGURE 15. FILLING (A) AND TAGGING (B) OF THE MOLDS WITH THE FABRICATED CONCRETE

For the curing of the concrete specimens, the molds are transported to the humidity chamber, or curing chamber (Figure 16) at Promsa where they are stored at a 20 +/- 1 ºC temperature and a relative humidity no smaller than 95%. It is important to mention that before the specimens are stored, they remain inside their molds for 24 hours in order to avoid dehydration and carefully covered in order to avoid direct sunlight contact.

FIGURE 16. CURING CHAMBER

Once 28 days had gone by and the concrete had reached its characteristic strength, the specimens were taken back to the UPC Campus Nord laboratory. They were then stored in a freezer until they reached the designated temperature (-30, -20 or -10 ºC) prior to being tested. (Figure 17)

FIGURE 17. SPECIMENS DEPOSITED INSIDE THE FREEZER

3.6 Fresh Concrete Tests

As it has been mentioned previously, in order to determine the workability of the mix and to find out if it is adequate, after concrete mixing, a sample is taken from each dose in order to determine its consistency.

FIGURE 18. SLUMP TEST

The consistency can be obtained by the Slump Test (UNE 83313), which consists in filling up a truncated cone- shaped mold and removing it once filled up completely (Figure 18). Once the concrete is out of the mold it starts to settle more or less depending on its consistency. The measurement of the settlement of the concrete in centimeters is referred to as the slump test settlement.

The occluded air inside fresh concrete is carried out according to UNE 83315. For this test, an occluded air measuring device is used which basically introduces pressured air inside a clamped cylindrical container which contains a concrete sample submerged in water. Given the compressibility of air, when the pressure is increased, the volume of air trapped inside the sample diminishes and the water level decreases. This decrease in water level due to the introduced pressure indicates the volume of air occluded inside the sample. The measuring device includes a graduated scale that shows the content of air in percentage for a determined pressure applied (kg/cm2) (Figure 19).

FIGURE 19. OCCLUDED AIR MEASURING DEVICE

The last test carried out on fresh concrete was the determination of the specimen density. This test follows the UNE 83317 norm. A rigid and watertight mold is used with the smallest size no smaller than 10 cm or four times the maximum aggregate size. The capacity as well as its mass are determined with an error of about 0,1%. Once the mold is filled up according to the same specifications indicated beforehand, it is weighed (m_2) and consecutively subtracted the initial weight of the mold (m_1). Once the mass has been determined, it is then divided by the total volume of the mold (V) thus obtaining the density (ρ), expressed in kg/m3 in eq. (1).

$$\rho = \frac{(m_2 - m_1)}{V} \qquad (1)$$

3.7 Hardened Concrete Test (3-Point-Bending Test)

Tensile behavior in concrete with fibers is evaluated in terms of the residual strength due to bending, determined by the load-displacement curve at the edge of the crack via the three-point bending test.

This test consists in applying a load via a centered rolling pin on a prismatic specimen (600x150x150mm). The specimen is supported by two pins on each side separated by 500 mm. Halfway through this separation, the specimen has a 25 mm-deep notch. This, as explained previously, provides crack width and quantity control when loaded. The pins, 2 of three of which are mobile (including the upper pin), consist of a 30 +/- 1 mm diameter and are made of steel.

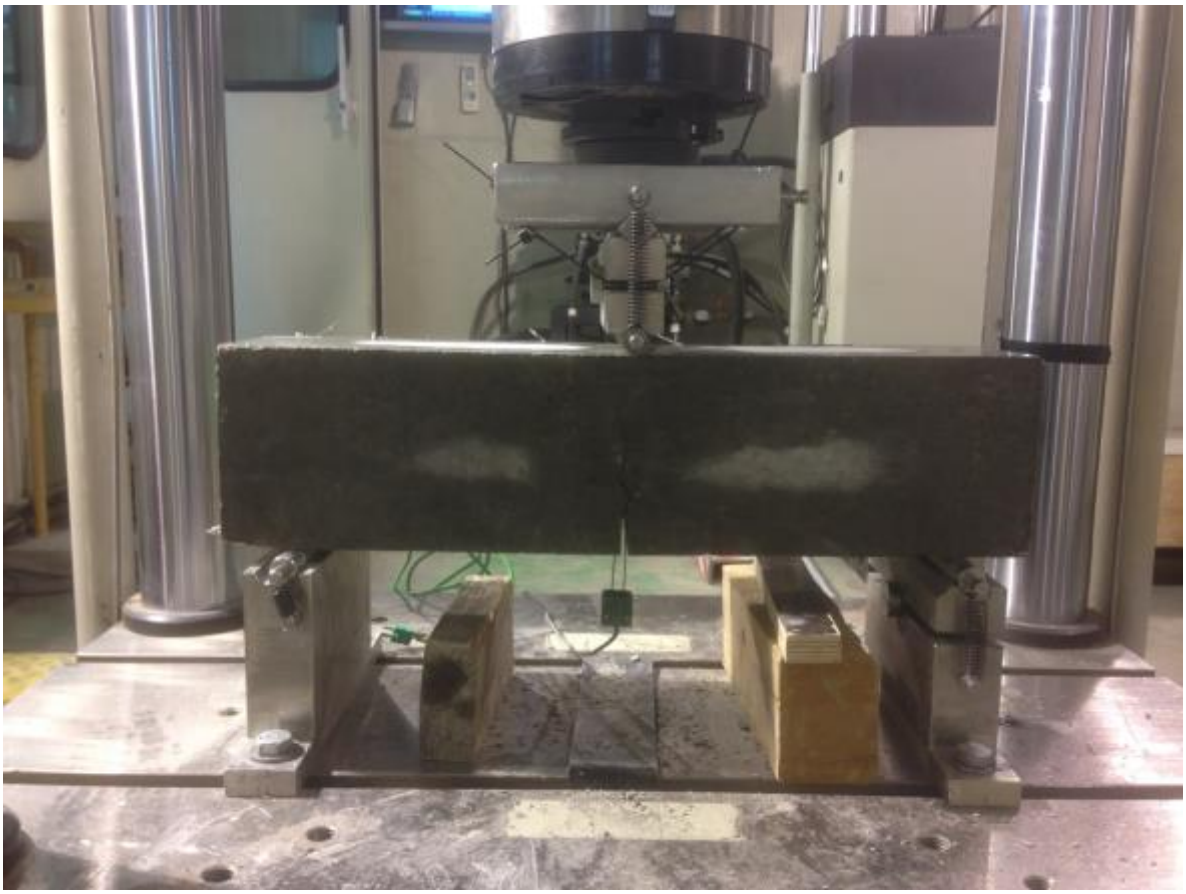

FIGURE 20. THREE-POINT BENDING TEST

The notch, apart from locating cracking in the section, also aims to avoid dispersions in results, which are already important in fiber-reinforced concrete. This allows that, if the load is centered, the maximum bending moment to match the vertical area that passes through the application point, which would only affect the concrete under it.

FIGURE 21. CARRYING OUT THE NOTCH ON THE SPECIMENS

In order to measure the displacement of the border of the notch, a measuring device is installed at the center. This device is connected to a data registering software, where the loads are registered with its corresponding CMOD.

FIGURE 22. MEASURING DEVICE TO REGISTER CMOD

CHAPTER IV

4. Analysis & Results

5.1 Introduction

In the last chapter, there was a big emphasis on the experimental campaign, the composition of the specimens and the techniques used for characterizing them. This chapter discusses the results of the different techniques explained for fresh-state concrete, as well as the three-point bending test in hardened concrete.

In order to have a better view of the results and how the object of study (freezing temperature) affects the elements, the present chapter will be organized in two main blocks.

- The first block discusses the results that have been able to been extracted from the tests as well as their characteristics.
- The second block compares the results obtained for elements submitted to freezing temperatures between themselves and to those which have been tested at room temperature.

Evidently, the major discussion topic in this chapter will be the three-point bending test and the reason for there being a difference in residual strength obtained for different doses and/or temperatures.

5.2 Objectives

The behavior that Plastic Fiber Reinforced Concrete (PFRC) present under freezing temperatures is still widely unknown. In this chapter, the aim is to carry out the following objectives:

- Characterize the behavior of PFRC under freezing phase in order to study the capability the fibers have to sew supposed cracks on external sides of the elements
- Study the weakening process, in terms of tensile strength, of the elements once they are frozen at different temperatures.

In the analysis of the results, the influence that load and pre-crack width have in long-term behavior on elements exposed to bending strengths must be evaluated firsthand. Taking this into account, this chapter focuses on two main results: Crack Mouth Opening Displacement (CMOD) and residual strength, which is the mechanical capacity that the elements possess once cracked. Residual strength was obtained for different CMODs in order to help observe difference in results:

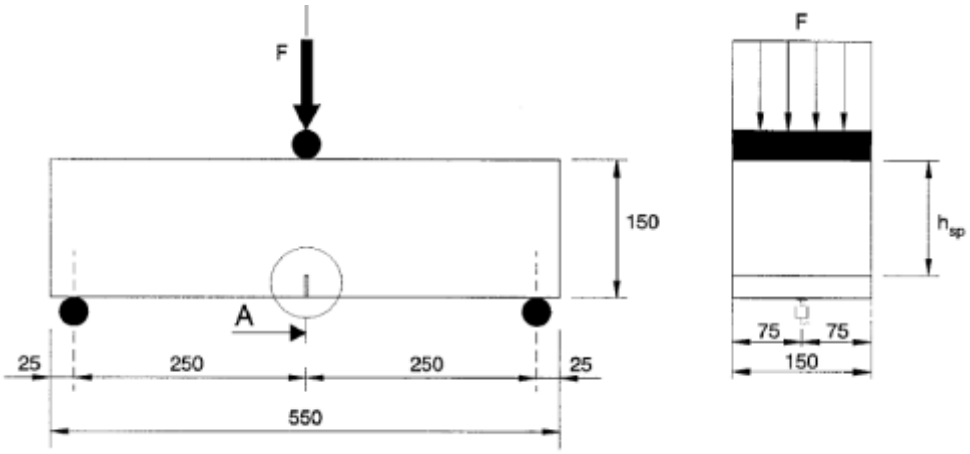

FIGURE 23. THREE-POINT BENDING TEST SCHEME

$CMOD_1$ = 0,5 mm

$CMOD_2$ = 1,5 mm

$CMOD_3$ = 2,5 mm

$CMOD_4$ = 3,5 mm

As mentioned before, this test is aimed towards FRC with notches or initial cracks where behavior is exclusively ruled by cracking. Deformation is therefore located at the edge of the notch and, due to crack propagation, in the crack surroundings. In the 3-point

Bending Test, where specimens have previously been marked with a notch, the most important deformation is the crack itself and therefore the best variable in order to control it is the crack mouth opening displacement mentioned earlier (CMOD) or a similar displacement.

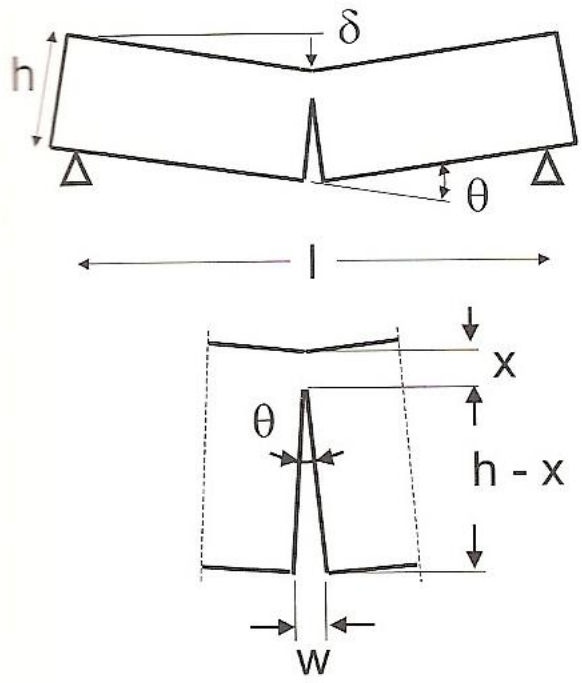

FIGURE 24. RELATION BETWEEN CRACK WIDTH AND SPECIMEN DEVIATION

The notch has the advantage of allowing CMOD to control displacement evolution. In this line of work, it will be interesting to observe graphs relating CMOD to load applied, as well as the approximate relation between CMOD and deviation:

$$\delta = 0{,}85\ CMOD + 0{,}04 \qquad (2)$$

Where:

δ is deviation, in mm

$CMOD$ is crack mouth opening displacement, in mm.

Once these graphs are obtained for each of the doses, observations were able to be made in order to deduct certain behavior patterns the specimens showed in testing. In

order to make comparisons between different temperatures and between room temperature, different campaigns were made for different temperature testing. These results in four different sections that this chapter will include:

- Specimens tested at -30ºC
- Specimens tested at -20ºC
- Specimens tested at -10ºC
- Specimens tested at +22ºC (room temperature)

In order to analyze residual flexural strength due to bending, the following formula (UNE-EN 14651) will be applied:

$$\boldsymbol{f_{R,j} = \frac{3F_j l}{2bh_{sp}^2}} \qquad (3)$$

Where:

$f_{R,j}$: residual strength due to bending corresponding to $CMOD = CMOD_j$.

F_j : load corresponding to $CMOD = CMOD_j$.

l : length of the span, in millimeters.

b : width of the specimen, in millimeters.

h_{sp}: distance between the end of the notch and upper part of the specimen, in millimeters.

Each of the results will be introduced and consecutively explained in its corresponding section.

5.3 Specimens tested at -30ºC

For this temperature, three different samples were tested in order to have a broader view of results and to better evaluate the possible inconsistencies between them. The specimens were placed inside the refrigerator until the temperature transducers indicated the totality of the prismatic element was at a -30ºC temperature.

The LOAD-CMOD graph that was elaborated given the results shows common traits for all three doses. Before cracking, they all consist of a linear-elastic behavior, as can be seen in conventional concrete, given the fact that in this phase the fibers have not started to carry out their function and mechanical behavior is not significantly modified. Once this first crack has appeared, and therefore the fibers start to contribute in mechanical behavior,

the concrete starts to transfer the load to the fibers, which resist cracking due to their adherence to the concrete matrix.

Therefore, after the first crack, the load needed in order to increase CMOD decreases until it reaches a minimum value which is associated with the decrease in stiffness result of the cracking. At this point, the opposite effect occurs: once the fibers start acting carrying out their bridge effect (sewing) and thus contributing to the specimen's ductility, the load needed in order to increase CMOD increases.

FIGURE 25. TEST PERFORMED TO -30ºC SPECIMEN

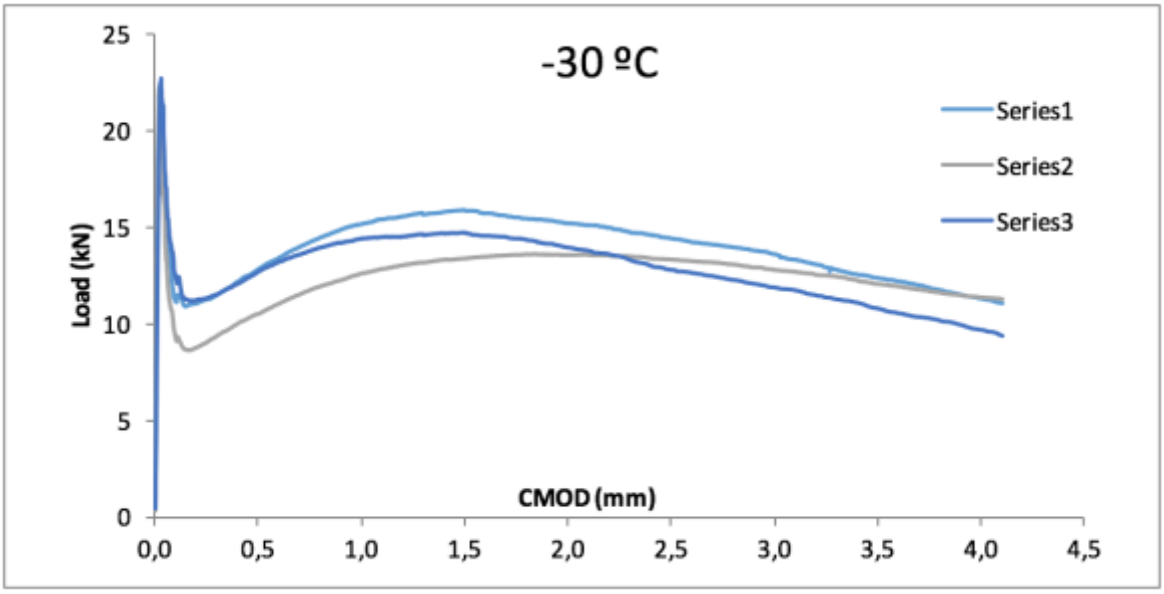

FIGURE 26. LOAD-CMOD GRAPH FOR -30ºC SPECIMENS

With the span length being $l = 600 - 25 - 25 = 500\ mm$, a base of $b = 150\ mm$ and $h_{sp} = 150 - 25 = 125\ mm$, we can easily obtain the residual strengths for each of the CMODs mentioned above.

When CMOD was at 0,5 mm, the load applied was between 10 and 13 kN for all three samples, resulting in an average residual strength of 3,85 MPa. For CMOD of 1,5 mm, the load increased up to 13 -16 kN resulting in an average of 4,68 MPa.

At 2,5 mm, we see a slight decrease of the admitted load, which drops to 12-15 kN with an average residual strength of 4,32 MPa. This is to be expected, given the visible peak that can be seen on the graph between 1,5 and 2,5 mm. Finally, for CMOD of 3,5 mm we find a larger decrease with an applicable load of 10 to 12 MPa and an average residual strength of 3,75 MPa.

As for the maximum values registered pre-crack, it was found that the maximum residual strength was shown for a 22 to 23 kN load, resulting in an average residual strength of 7,15 MPa.

These results are summarized in the following tables for each one of the samples tested:

	CMOD (mm)	**0,5**	**1,5**	**2,5**	**3,5**
S_1	**Load**	12,85	15,85	14,41	12,36
	$f_{R,1}$	4,11	5,07	4,61	3,95
S_2	**Load**	10,47	13,35	13,3	12,03
	$f_{R,2}$	3,35	4,27	4,26	3,85
S_3	**Load**	12,75	14,72	12,79	10,79
	$f_{R,3}$	4,08	4,71	4,09	3,45
Average	f_R	**3,85**	**4,68**	**4,32**	**3,75**

TABLE 6. RESULTS REGARDING LOAD AND RESIDUAL FLEXURAL STRENGTH

5.4 Specimens tested at -20ºC

For this temperature, three different samples were tested in order to have a broader view of results and to better evaluate the possible inconsistencies between them. The specimens were placed inside the refrigerator until the temperature transducers indicated the totality of the prismatic element was at a -20ºC temperature.

The LOAD-CMOD graph that was elaborated given the results shows common traits for all three doses. Before cracking, they all consist of a linear-elastic behavior, as can be seen in conventional concrete, given the fact that in this phase the fibers have not started to carry out their function and mechanical behavior is not significantly modified. Once this first crack has appeared, and therefore the fibers start to contribute in mechanical behavior, the concrete starts to transfer the load to the fibers, which resist cracking due to their adherence to the concrete matrix, resisting approximately the initial strength reached.

Therefore, after the first crack, the load needed in order to increase CMOD decreases until it reaches a minimum value which is associated with the decrease in stiffness result of the cracking. At this point, the opposite effect occurs: once the fibers start acting carrying out their bridge effect (sewing) and thus contributing to the specimen's ductility, the load needed in order to increase CMOD increases.

FIGURE 27. TEST PERFORMED TO -20ºC SPECIMEN

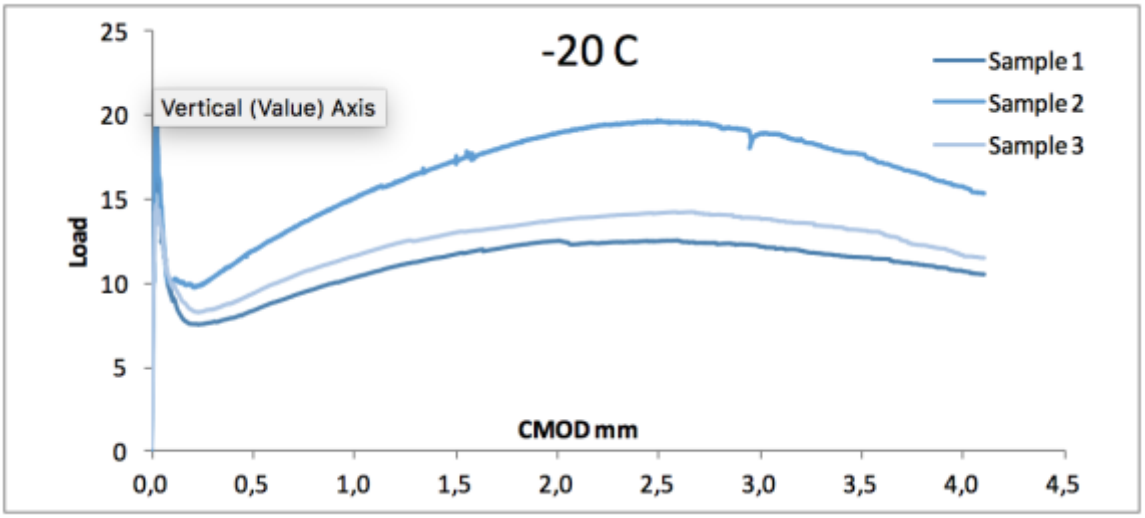

FIGURE 28. LOAD-CMOD GRAPH FOR -20ºC SPECIMENS

With the span length being $l = 600 - 25 - 25 = 500\ mm$, a base of $b = 150\ mm$ and $h_{sp} = 150 - 25 = 125\ mm$, we can easily obtain the residual strengths for each of the CMODs mentioned above.

When CMOD was at 0,5 mm, the load applied was between 8 and 12 kN for all three samples, resulting in an average residual strength of 3,38 MPa. For CMOD of 1,5 mm, the load increased up to 11 -18 kN resulting in an average of 4,80 MPa.

At 2,5 mm, we see a slight increase of the admitted load, which rises up to 12-20 kN with an average residual strength of 5,25 MPa. Finally, for CMOD of 3,5 mm we find a larger decrease with an applicable load of 1 to 18 MPa and an average residual strength of 4,81 MPa. This is to be expected, given the visible peak that can be seen on the graph between 2,5 and 3,5 mm which almost reaches the initial strength observed before cracking.

As for the maximum values registered pre-crack, it was found that the maximum residual strength was shown for a 15 to 20 kN load, resulting in an average residual strength of 6,10 MPa. These results are summarized in the following tables for each one of the samples tested:

	CMOD (mm)	**0,5**	**1,5**	**2,5**	**3,5**
S_1	**Load**	8,39	11,74	12,50	11,55
	$f_{R,1}$	2,85	3,98	4,24	3,92
S_2	**Load**	11,96	17,61	19,63	17,74
	$f_{R,2}$	4,06	5,97	6,66	6,02
S_3	**Load**	9,42	13,02	14,18	13,15
	$f_{R,3}$	3,22	4,46	4,85	4,50
Average	f_R	**3,38**	**4,80**	**5,25**	**4,81**

TABLE 7. RESULTS REGARDING LOAD AND RESIDUAL FLEXURAL STRENGTH

5.5 Specimens tested at -10ºC

For this temperature, two different samples were tested in order to have a broader view of results and to better evaluate the possible inconsistencies between them. The specimens were placed inside the refrigerator until the temperature transducers indicated the totality of the prismatic element was at a -10ºC temperature.

The LOAD-CMOD graph that was elaborated given the results shows common traits for all two doses. Before cracking, they both consist of a linear-elastic behavior, as can be seen in conventional concrete, given the fact that in this phase the fibers have not started to carry out their function and mechanical behavior is not significantly modified. Once this first crack has appeared, and therefore the fibers start to contribute in mechanical behavior, the concrete starts to transfer the load to the fibers, which resist cracking due to their adherence to the concrete matrix.

Therefore, after the first crack, the load needed in order to increase CMOD decreases until it reaches a minimum value which is associated with the decrease in stiffness result of the cracking. At this point, the opposite effect occurs: once the fibers start acting carrying out their bridge effect (sewing) and thus contributing to the specimen's ductility, the load needed in order to increase CMOD increases, reaching a higher strength than the one observed before the first crack.

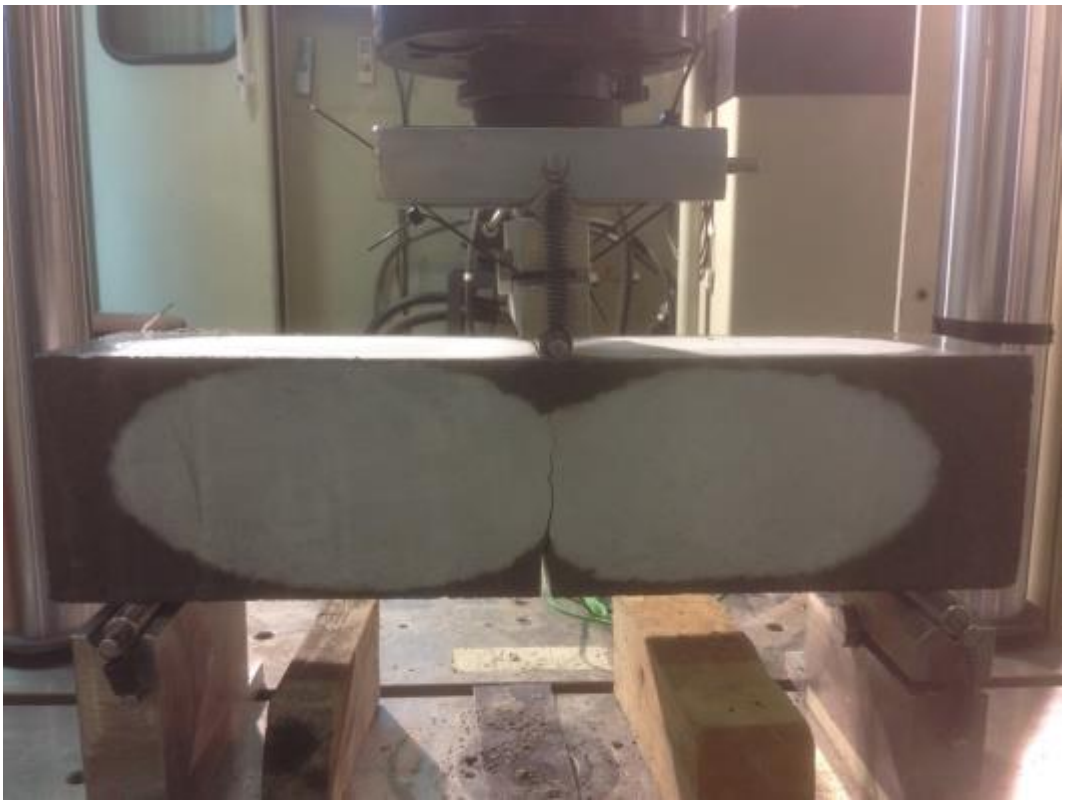

FIGURE 29. TEST PERFORMED TO -10ºC SPECIMEN

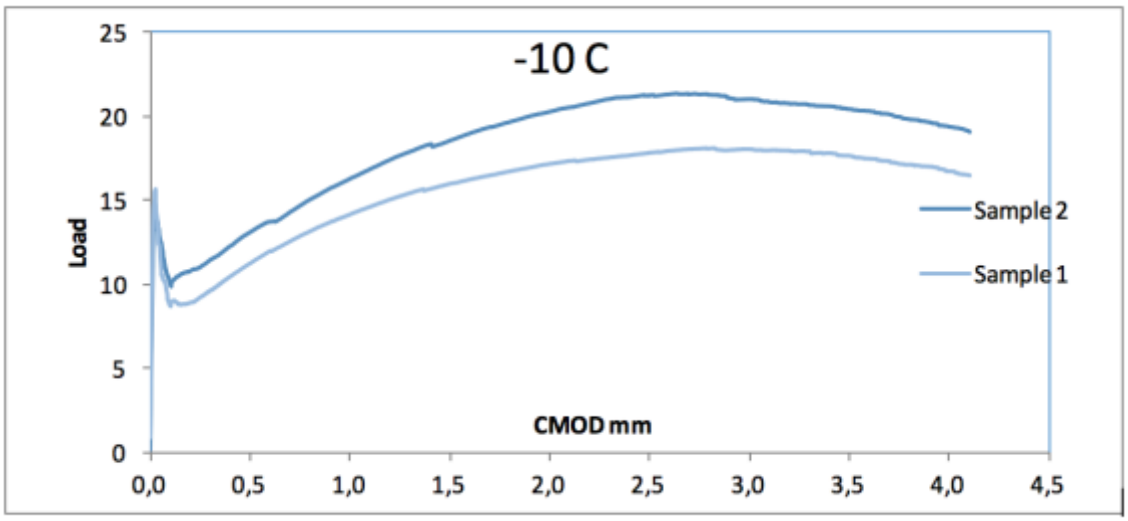

FIGURE 30. LOAD-CMOD GRAPH FOR -20ºC SPECIMENS

With the span length being $l = 600 - 25 - 25 = 500\ mm$, a base of $b = 150\ mm$ and $h_{sp} = 150 - 25 = 125\ mm$, we can easily obtain the residual strengths for each of the CMODs mentioned above.

When CMOD was at 0,5 mm, the load applied was between 11 and 13 kN for all three samples, resulting in an average residual strength of 4,11 MPa. For CMOD of 1,5 mm, the load increased up to 16 -18 kN resulting in an average of 5,83 MPa.

At 2,5 mm we can observe load capacity increases even more, up to 17-21 kN, with an average residual strength of 6,59 MPa. Finally, for CMOD of 3,5 mm we find that load capacity decreases slightly with an applicable load of about 17 to 20 MPa and an average residual strength of 6,43 MPa. This is to be expected, given the visible peak that can be seen on the figure 30 between 2,5 and 3,5 mm which reaches even a greater load capacity than that observed pre-cracking.

As for the maximum values pre-crack registered, it was found that the maximum residual strength was shown for a 15 to 18 kN load, resulting in an average residual strength of 5,71 MPa.

These results are summarized in the following tables for each one of the samples tested:

	CMOD (mm)	**0,5**	**1,5**	**2,5**	**3,5**
S_1	**Load**	11,28	16,03	17,89	17,72
	$f_{R,1}$	3,83	5,44	6,07	6,01
S_2	**Load**	13,08	18,53	21,20	20,42
	$f_{R,2}$	4,39	6,22	7,11	6,85
Average	f_R	**4,11**	**5,83**	**6,59**	**6,43**

TABLE 8. RESULTS REGARDING LOAD AND RESIDUAL FLEXURAL STRENGTH

5.6 Specimens tested at room temperature

For this temperature, three different samples were tested in order to have a broader view of results and to better evaluate the possible inconsistencies between them. In this case, the specimens weren't placed inside the freezer once fabricated as was done for all other specimens in order to test them at room temperature, at approximately 22 ºC.

The LOAD-CMOD graph that was elaborated given the results shows common traits for all three doses. Before cracking, they all consist of a linear-elastic behavior, as can be seen in conventional concrete, given the fact that in this phase the fibers have not started to realize their function and mechanical behavior is not significantly modified. Once this first crack has appeared, and therefore the fibers start to contribute in mechanical behavior, the concrete starts to transfer the load to the fibers, which resist cracking due to their adherence to the concrete matrix.

Therefore, after the first crack, the load needed in order to increase CMOD decreases until it reaches a minimum value which is associated with the decrease in stiffness result of the cracking. At this point, the opposite effect occurs: once the fibers start acting carrying out their bridge effect (sewing) and thus contributing to the specimen's ductility, the load needed in order to increase CMOD increases.

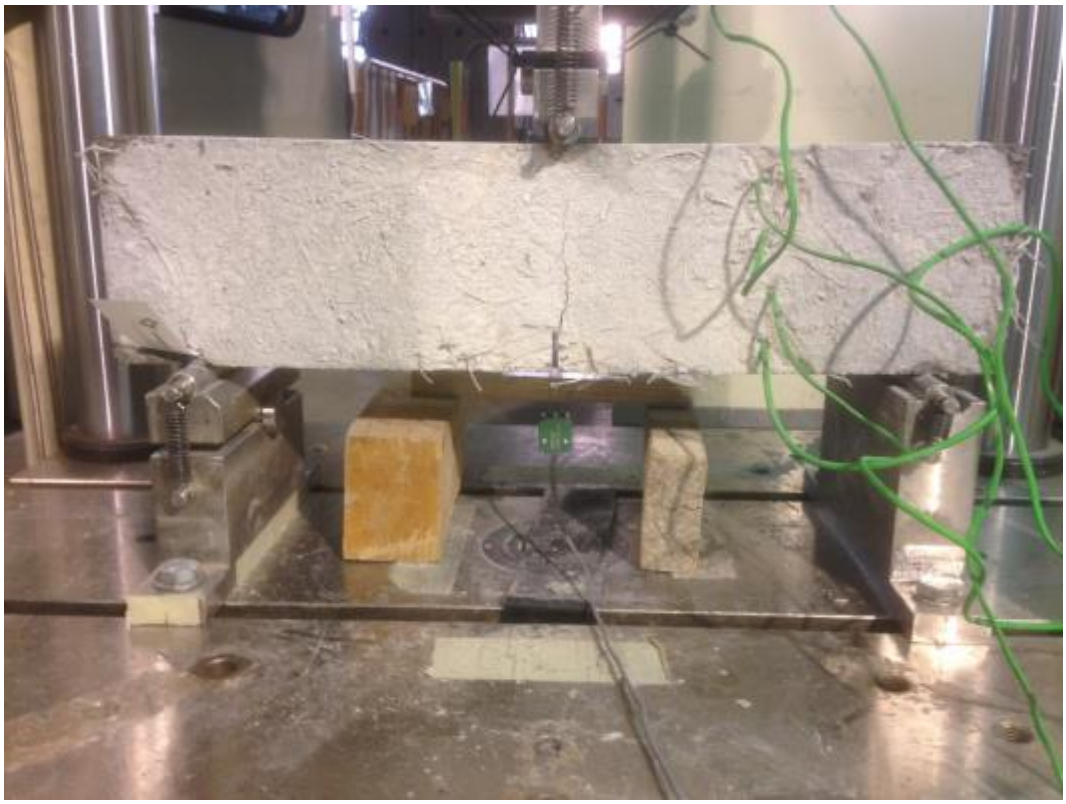

FIGURE 31. TEST PERFORMED TO ROOM TEMPERATURE SPECIMEN

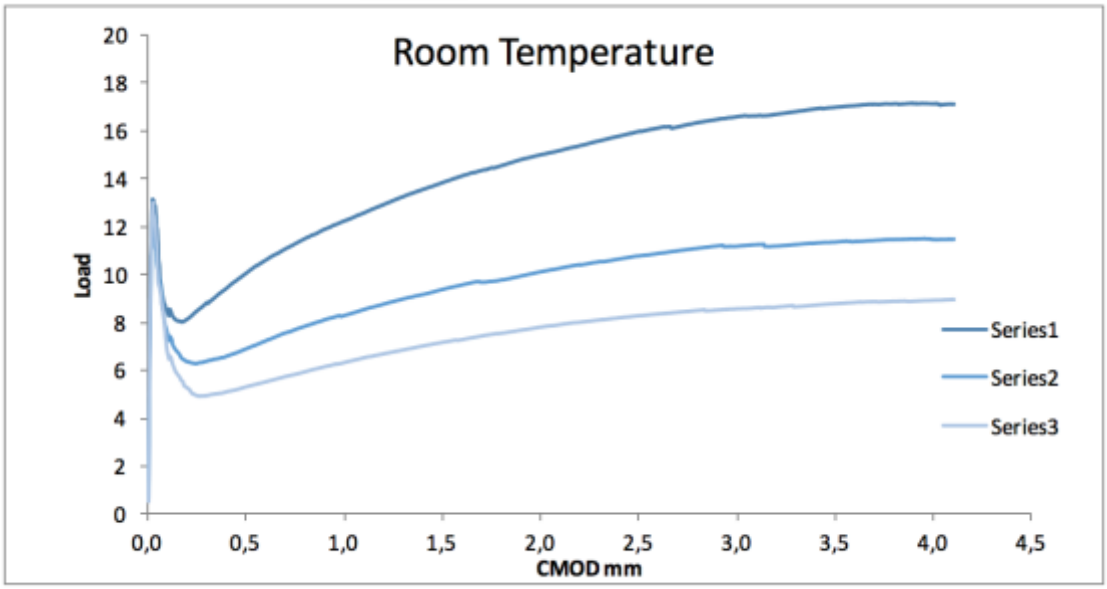

FIGURE 32. LOAD-CMOD GRAPH FOR ROOM TEMPERATURE SPECIMENS

With the span length being $l = 600 - 25 - 25 = 500\ mm$, a base of $b = 150\ mm$ and $h_{sp} = 150 - 25 = 125\ mm$, we can easily obtain the residual strengths for each of the CMODs mentioned above.

When CMOD was at 0,5 mm, the load applied was between 5 and 10 kN for all three samples, resulting in an average residual strength of 2,38 MPa. For CMOD of 1,5 mm, the load increased up to 7 -14 kN resulting in an average of 3,24 MPa.

At 2,5 mm, we continue to see an increase of the admitted load, which rises up to 8-16 kN with an average residual strength of 3,74 MPa. Finally, for CMOD of 3,5 mm we find another increase with an applicable load of up to 17 MPa and an average residual strength of 3,96 MPa.

As for the maximum values registered pre-crack, it was found that the maximum residual strength was shown for a 12 to 13 kN load, resulting in an average residual strength of 4,13 MPa.

These results are summarized in the following tables for each one of the samples tested:

	CMOD (mm)	**0,5**	**1,5**	**2,5**	**3,5**
S_1	**Load**	10,10	13,86	16,01	17,01
	$f_{R,1}$	3,23	4,44	5,12	5,44
S_2	**Load**	6,92	9,40	10,80	11,38
	$f_{R,2}$	2,22	3,01	3,46	3,64
S_3	**Load**	5,30	7,15	8,26	8,75
	$f_{R,3}$	1,69	2,29	2,64	2,80
Average	f_R	**2,38**	**3,24**	**3,74**	**3,96**

TABLE 9. RESULTS REGARDING LOAD AND RESIDUAL FLEXURAL STRENGTH

5.7 Analysis of Results

This section of the chapter aims to analyze the relation certain variables may have when exposed to extremely cold temperatures. One interesting analysis to be made, is the maximum load the specimens were able to resist before their first crack.

Figure 33 shows the maximum load capacity observed in each of the samples of the specimens. It should be noted that this refers to the maximum load that was observed before the first crack appeared.

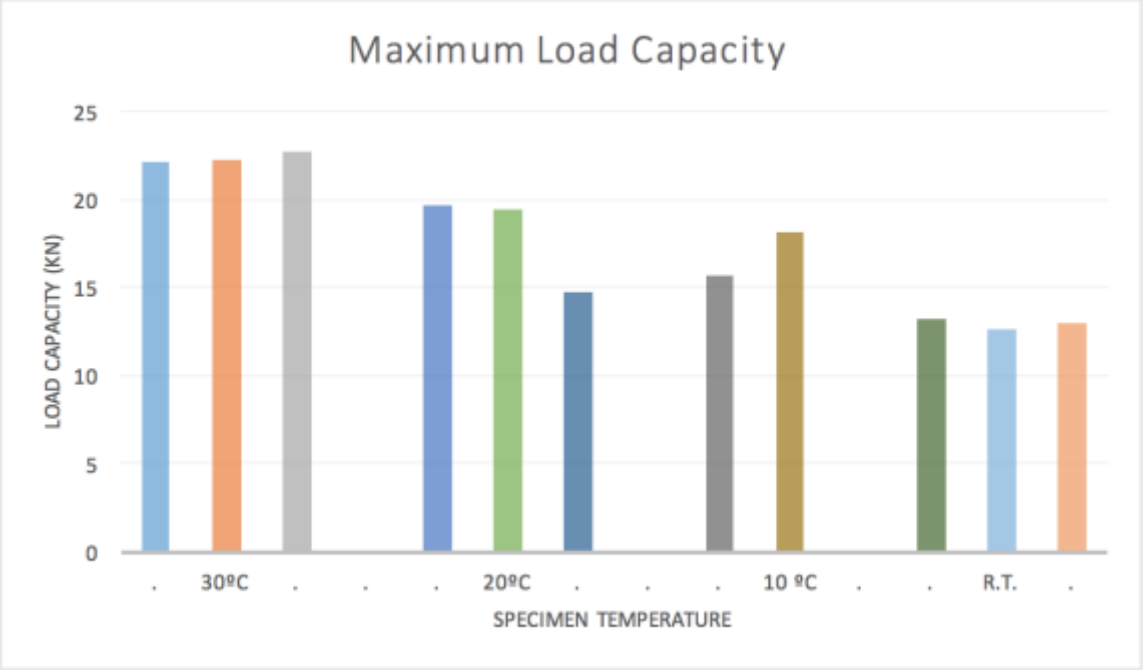

FIGURE 33. GRAPH RELATING LOAD CAPACITY TO SPECIMEN TEMPERATURE

As can be seen in the figure 33, the three samples of each of the temperatures (except -10 ºC which has two samples instead of three) show a clear tendency that for lower temperature, pre-crack load capacity seems to be higher than for higher ones. This can be seen in a nearly 80% increase in load capacity from -30 ºC (22,06 kN) to room temperature (13,16 kN).

With this information, it can be extracted that pre-crack performance (in terms of load capacity) generally improves for freezing conditions rather than for above 0ºC temperatures; that is: concrete strength increases as temperature is lowered, basically due to moisture content, among others.

In the LOAD-CMOD graphs shown previously, it can also be observed that pre-crack behavior was not the only modified variable.

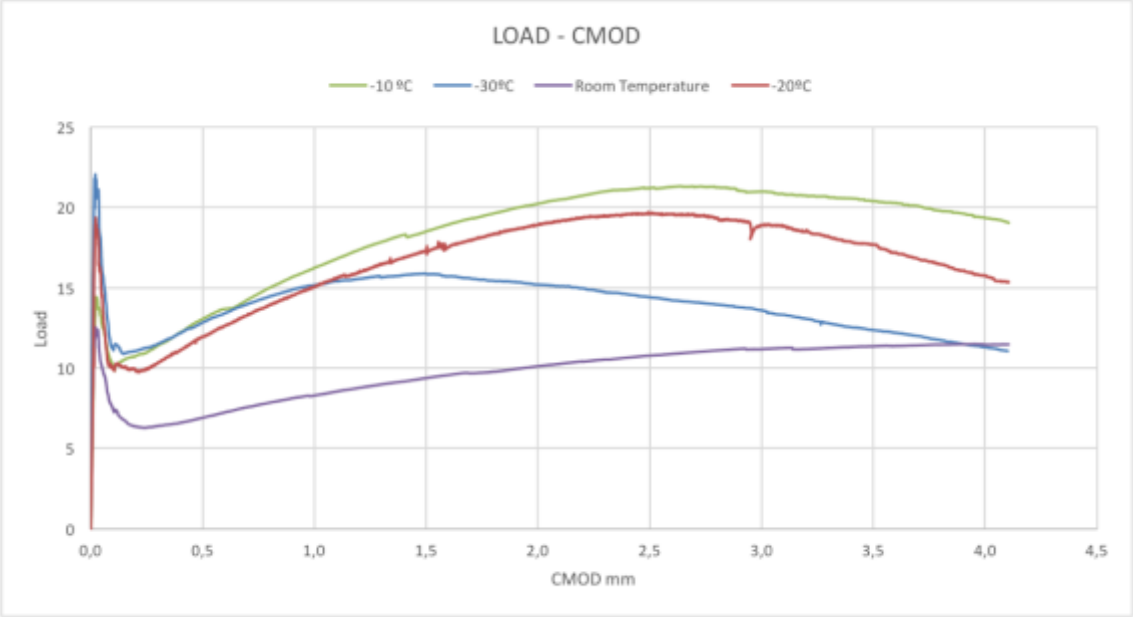

FIGURE 34. COMPOUND GRAPH OF AVERAGE OF ALL SPECIMENS TESTED

One of the most interesting effects observed in this experimental campaign is the change in residual strength throughout temperature variation. Residual strength is that which the specimen possesses once it has fractured, linking it to ductility and consequently to durability as well. This phenomenon is interesting and important in this framework due to the importance that durability has in tunnel lining construction.

Temperature	f_{max}	$f_{w=0,5}$	$f_{w=1,5}$	$f_{w=2,5}$	$f_{=3,5}$
-30 ºC	7,15	3,85	4,68	4,32	3,75
-20 ºC	6,10	3,38	4,80	5,25	4,81
-10 ºC	5,71	4,11	5,83	6,59	6,43
22 ºC	4,13	2,38	3,24	3,74	3,96

TABLE 10. RESIDUAL STRENGTH IN RELATION WITH TEMPERATURE

Figure 34 shows how residual strength improves as temperature decreases, which is in part due to the increase of volume in pores due to internal water freezing, generating certain expansion in the matrix and consequently compressing fibers (more on this below).

As can be seen (chart), although specimens tested at -30 ºC show the greatest initial residual strength, specimens tested at -10 ºC show greater strength at the focused crack openings.

In comparison to the other freezing-temperature-tested specimens and to the room-temperature-tested specimen, the ones tested at -10 ºC demonstrated an increase in residual flexural strength of the following percentages for each of the focused crack openings:

Temperature	$f_{w=0,5}$	$f_{w=1,5}$	$f_{w=2,5}$	$f_{=3,5}$
-30 ºC	6,74%	24,41%	52,54%	71,34%
-20 ºC	21,66%	21,28%	25,49%	33,61%
+22 ºC	72,52%	79,65%	76,18%	62,31%

TABLE 11. INCREASES IN RESIDUAL FLEXURAL STRENGTH REGARDING SPECIMENS TESTED AT -10 ºC

This shows an increase in residual flexural strength of up to almost 80% (from -10 ºC to +22ºC). Related to residual flexural strength, it is also an interesting observation to note the load capacity recovery once the first crack appears on the specimen. As seen on the graphs, there is a clear relation between the load capacity peaks presented post-crack and the temperature in which the specimens were tested.

The most prevailing deduction as to why this increase in residual strength is observed in the graphs presented can be the physical alterations the element suffers once temperature reaches a certain level below zero.

Influence in fiber-concrete interaction un sub-zero temperature is surely to contribute to the increase in residual flexural strength. By observing the results obtained in the graphs and by recalling the previously mentioned statement in Chapter 3 – State of the Art:

> *Between 20 ºC and -15 ºC, concrete contracts.*
>
> *Between -20 ºC and -60 ºC concrete expands. This is called the transition region and can be explained by taking into account the gradual transformation of water into ice on concrete pores*

Another interesting conclusion can be deduced. The following graph, included previously in this same thesis, shows the different residual flexural strengths present in the specimens which were tested in different temperatures:

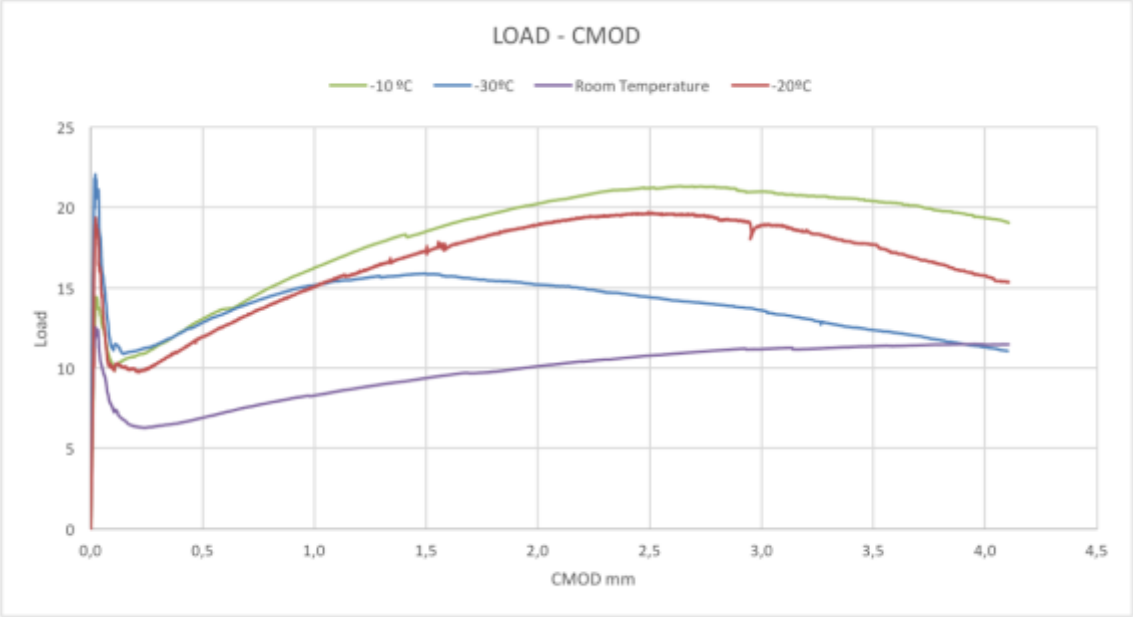

FIGURE 35. COMPOUND GRAPH OF AVERAGE OF ALL SPECIMENS TESTED

As can be seen, fibers tested at -10 ºC present the major increase in residual flexural strength, followed by specimens tested at -20 ºC and lastly by specimens tested at -30 ºC. This effect can be directly related to concrete behavior under freezing temperatures as explained previously (M. Calafat, 1982).

The pull-out failure mode in FRC is one of the most typical failure mechanisms for elements fabricated with this type of concrete.

Some load transfer between fibre and matrix is still possible after debonding by interfacial forces due to matrix shrinkage onto the fibre during manufacture. This friction produces a

non-uniform stress along the debonded fibre. Because of the variable strength of the fibre along its length the fibre is able to break some distance from the matrix crack-plane where the stress is highest. After fracture, the composite typically shows a matrix crack-plane with fibres protruding from it. This is called pull-out. (J.K. Wells, 1984)

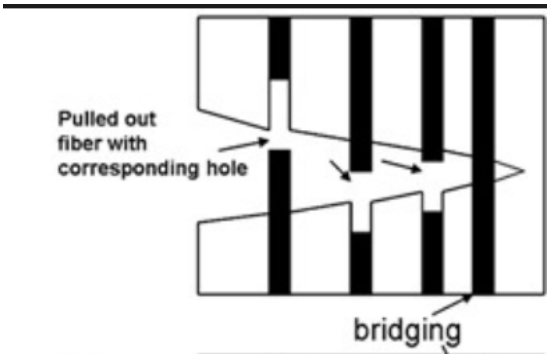

FIGURE 36. REPRESENTATION OF FIBER PULL-OUT MECHANISM AND BRIDGING EFFECT (MENG, 2015)

Concrete contraction can lead to better adherence between the fiber and cementitious matrix due to greater contact between the two elements. This would in turn make the pull-out load failure less probable to happen and favor the bridging effect between fiber and matrix, which would explain the increase in residual strength and permit a more ductile failure to occur.

Furthermore, as temperature continues to decrease past -15 ºC, the expansion produced in the pores would debilitate the adherence between the matrix and the fiber and therefore facilitate the pull-out mechanism.

This can be corroborated by figure 35 in which specimens tested increase their residual flexural strength gradually as temperature is lowered (-10 ºC and -20 ºC tested specimens which correspond to a contraction in the pores) and then starts to lower once again as temperature continues to decrease (-30 ºC tested specimen which correspond to an expansion in the pores).

In order to better understand the evolution of residual flexural resistance throughout different freezing temperatures, the following figures have been presented for serviceability limit state (SLS), which corresponds to residual flexural resistance for crack openings of 0,5 mm and ultimate limit state (ULS) which corresponds to residual flexural resistance for crack openings of 2,5 mm.

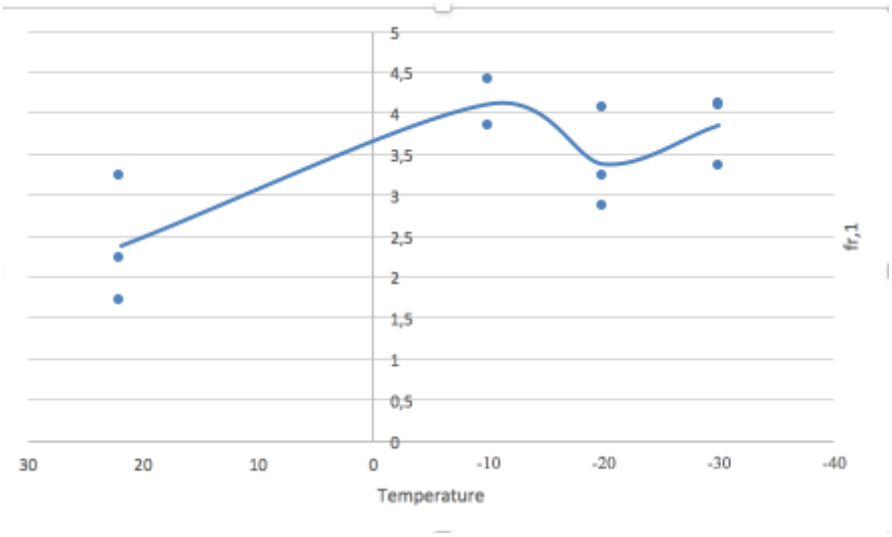

FIGURE 37. RESIDUAL FLEXURAL STRENGTH FOR SERVICEABILITY LIMIT STATE (SLS)

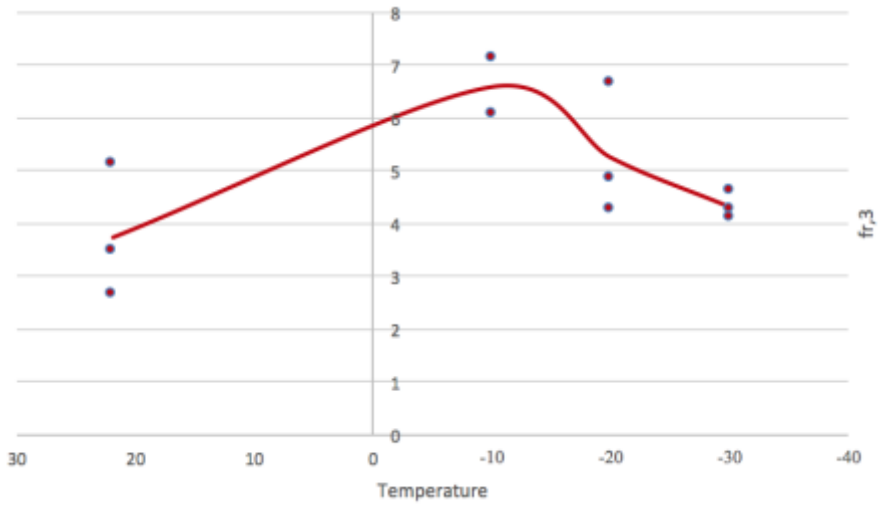

FIGURE 38. RESIDUAL FLEXURAL STRENGTH FOR ULTIMATE LIMIT STATE (ULS)

These figures clearly state how cooling processes affect residual flexural strength in a positive manner. In ELS, fibers are able to achieve greater residual strengths than specimens tested at room temperature. The same can be said for ULS, where they also reach higher values than those tested at room temperature. This can be a very relevant observation, since tunnel segments are critically strict on crack opening restrictions.

CHAPTER V

5. Conclusions & Future Studies

5.1 Introduction

In this research document, the main objective was to observe how Plastic Fiber Reinforced Concrete behaved under certain temperatures and, more specifically, under the cooling processes that TBM segments undergo. The most critical moment in their fabrication procedure is during the steam curing process, which is when the elements are submitted to the greatest temperature differentials. It is mainly during this phase in which cracking is prone to appear and for which this study has focused its principles.

Therefore, the aim of this thesis has been to study the behavior that Plastic Fiber Reinforced Concrete has when submitted to cooling processes for the design of TBM segments in countries that harbor extreme sub-zero temperatures.

In order to carry out this research document, the first approach was to contextualize it by explaining the processes TBM segments are subjected to and how they are prone to crack due to the high temperature gradients.

Once the objective was clear, an experimental campaign was introduced with the objective of understanding the behavior PFRC has under these conditions.

Finally, the tests carried out on the PFRC specimens were analyzed in order to extract a coherent behavior pattern that the elements would present.

5.2 Conclusion

The conclusion that this thesis offers has much to do with residual flexural strength. Once the first crack appears, the fibers start to carry out their functions to bridge together the concrete that tends to crack due to tensile stress. The reachable strength once concrete has cracked can give us an overview of the way fibers contribute to in concrete.

Furthermore, load capacity before the first crack appears is also an important trait in this line of study, given the importance durability has in TBM segments.

In this thesis, it was found that as temperature decreased and pores contracted, the residual flexural strength increased. This increase continued until the temperature reached -20 ºC, in which internal pores would start to expand once again and the adherence with the fibers became weaker.

Load capacity was also found to increase as temperature decreased past room temperature, showing the greatest load capacity at the lowest temperature tested, -30 ºC. This trait reached almost an 80% increase regarding specimens tested at room temperature, which emphasizes the outstanding behavior plastic fibers have demonstrated to have in these sub-zero temperatures.

For this reason and in comparison with specimens tested at room temperature, the study was able to conclude that PFRC, when submitted to sub-zero temperatures:

- Shows greater load capacity (reaching almost and 80% increase) than that shown when tested at room temperature, as temperature decreases until -20 ºC (temperature in which it starts to decrease once again).

- Is able to resist greater loads before giving in to the first crack as temperature decreases from room temperature until the lowest temperature tested, -30 ºC.

5.3 Future Line of Studies

In order to compliment this study, it would be interesting to see how these types of fibers behave singularly when submitted to the same temperatures in order to compare the results to the ones exposed in this thesis. Indeed, tensile behavior, Poisson coefficient and other mechanical traits would be helpful in defining the overall behavior TBM segments will have in these conditions.

References.

Kim, D.J., Park, S.H., Ryu, G.S. and Koh, k.t., 2011. Comparative flexural behavior of hybrid ultra-high-performance fiber reinforced concrete with different macro fibers. Construction and building materials, 25(11), pp.4144-4155.

Zheng, Z. and Feldman, D., 1995. Synthetic fiber-reinforced concrete. Progress in polymer science, 20(2), pp.185-210.

Blontrock, H., Taerwe, L. and Matthys, s., 1999. Properties of fiber reinforced plastics at elevated temperatures with regard to fire resistance of reinforced concrete members. Special publication, 188, pp.43-54.

Bayasi, Z. and Zeng, J., 1993. Properties of polypropylene fiber reinforced concrete. Materials journal, 90(6), pp.605-610.

Juan Miquel Canet, (2006), Cálculo de Estructuras: Fundamentos y Estudio de Secciones, Ed. UPC.

Alhozaimy, A.M., Soroushian, P. and Mirza, F., 1996. Mechanical properties of polypropylene fiber reinforced concrete and the effects of pozzolanic materials. Cement and concrete composites, 18(2), pp.85-92.

Wang, Y., Li, V.C. and Backer, S., 1988. Modelling of fiber pull-out from a cement matrix. International journal of cement composites and lightweight concrete, 10(3), pp.143-149.

Literature Review on Macro Synthetic Fibres In Concrete Institute of Structural Engineering

Zhou, G. And Sim, L.M., 2002. Damage detection and assessment in fiber-reinforced composite structures with embedded fiber optic sensors-review. Smart materials and structures, 11(6), p.925.

Belletti B., Cerioni R., Meda A, Plizzari G. Design aspects on steel fiber-reinforced concrete pavements. J mater civ eng 2008;20(9):599–607.

Sorelli Lg, Meda A, Plizzari G. Steel Fiber Concrete Slabs on Ground: A Structural Matter. ACI STRUCT J 2006;103(4):551–8.

Ferrara L., Meda A. Relationships between fiber distribution, workability and the mechanical properties of SFRC applied to precast roof elements. 2006;39(288):411–20.

Zollo, r.f., 1997. Fiber-reinforced concrete: an overview after 30 years of development. Cement and concrete composites, 19(2), pp.107-122.

Soutsos, M.N., Le, T.T. and Lampropoulos, A.P., 2012. Flexural performance of fiber reinforced concrete made with steel and synthetic fibers. Construction and building materials, 36, pp.704-710.

Alberti, M.G., Enfedaque, A. and Gálvez, J.C., 2014. On the mechanical properties and fracture behavior of polyolefin fiber-reinforced self-compacting concrete. Construction and building materials, 55, pp.274-288.

Di Prisco, M., Plizzari, G. and Vandewalle, L., 2009. Fiber reinforced concrete: new design perspectives. Materials and structures, 42(9), pp.1261-1281.

EHE 08: fiber-reinforced concrete

Lawler, J.S., Zampini, D. and Shah, S.P., 2005. Microfiber and macro-fibre hybrid fibre-reinforced concrete. Journal of materials in civil engineering, 17(5), pp.595-604.
Wafa, F.F., 1990. Properties & applications of fibre reinforced concrete. Engineering sciences, 2(1).

Buratti, N., Mazzotti, C. and Savoia, M., 2011. Post-cracking behaviour of steel and macro-synthetic fibre-reinforced concretes. Construction and building materials, 25(5), pp.2713-2722.

Johnston, c.d., 2010. Fibre-reinforced cements and concretes (vol. 3). CRC press.
Caratelli, Angelo, et al. "structural behaviour of precast tunnel segments in fibre reinforced concrete." tunnelling and underground space technology26.2 (2011): 284-291.

Ritter, Klaus, Gerhard Ritter, and Klaus Matz. "Reinforcement Body for a Floor Slab." U.S. Patent no. 5,398,470. 21 Mar. 1995.

Grzybowski, M. and Shah, S.P., 1990. Shrinkage cracking of fibre reinforced concrete. Materials journal, 87(2), pp.138-148.

Cominoli, L., Failla, C. and Plizzari, G.A., 2007, June. Steel and Synthetic Fibres for Enhancing Concrete Toughness and Shrinkage Behaviour. In proceedings of international conference: sustainable construction materials and technologies (pp. 11-13).

Liao, L., de la Fuente, A., Cavalaro, s. and Aguado, A., 2015. Design of FRC tunnel segments considering the ductility requirements of the model code 2010. Tunnelling and underground space technology, 47, pp.200-210.

Soroushian, P. and lee, c.d., 1990. Distribution and orientation of fibres in steel fibre reinforced concrete. Materials journal, 87(5), pp.433-439.

Shah, S.P. and Rangan, B.V., 1971, February. Fibre reinforced concrete properties. In journal proceedings (vol. 68, no. 2, pp. 126-137).

Al Qadi, A.N. and Al-Zaidyeen, S.M., 2014. Effect of fibre content and specimen shape on residual strength of polypropylene fibre self-compacting concrete exposed to elevated temperatures. Journal of king Saud university-engineering sciences, 26(1), pp.33-39.

López-Buendía, A.M., Romero-Sánchez, M.D., Climent, V. and Guillem, C., 2013. Surface treated polypropylene (pp) fibres for reinforced concrete. Cement and concrete research, 54, pp.29-35.

Granju, Jean-Louis, and Sana Ullah Balouch. "corrosion of steel fibre reinforced concrete from the cracks." cement and concrete research 35.3 (2005): 572-577.

Poon, C.S., Shui, Z.H. and Lam, L., 2004. Compressive behaviour of fibre reinforced high-performance concrete subjected to elevated temperatures. Cement and concrete research, 34(12), pp.2215-2222.